From the Department of Neurobiology, Care Sciences and Society,
Division of Clinical Geriatrics,
Karolinska Institutet, Stockholm, Sweden

MAGNETIC RESONANCE STUDIES IN ALZHEIMER'S DISEASE

Eric Westman

Karolinska Institutet

Stockholm 2009

Published by Karolinska Institutet. Printed by Larserics Digital Print AB

ISBN 978-91-7409-624-8

Medicine is a science of uncertainty and an art of probability.

Sir William Osler

ABSTRACT

Alzheimer's disease (AD) is one of the most common forms of neurodegenerative disorders connected with gradual loss of cognitive functions such as episodic memory. The disease is related to pathological amyloid depositions and hyper phosphorilation of structural proteins in the brain which lead to progressive loss of function, metabolic alterations and structural changes in the brain. *In vivo* biomarkers need to be established to be able to set an early diagnosis, monitor disease progression and finally to observe pharmaceutical treatment effects. The aim of this thesis is to investigate the potential use of combining multivariate analysis with magnetic resonance imaging (MRI) and magnetic resonance spectroscopy (MRS) to monitor disease and treatment in AD. Due to the complexity of Alzheimer's disease, we hypothesized, that considering patterns of disease markers is more useful for the evaluation of patients or a study outcome, than making decisions based on single biomarkers alone.

Studies I and **II** combine multivariate analysis with MRS to monitor disease and treatment effects in two different mouse models. **Study III** utilizes multivariate analysis in combination with different MRI measures (regional and global volumetric and cortical thickness measures) to discriminate between three groups, AD patients, MCI patients and healthy controls. **Study IV** investigates the added value of MRS in the early diagnosis of AD. In this study the multivariate models were built combining both MRI and MRS variables.

The methods could successfully be applied in both animals and humans. Metabolic fingerprints of disease and treatment could be identified as well as patterns of atrophy. The combination of multivariate data analysis with different magnetic resonance measures is a powerful tool for identifying treatment effects and distinguishing between different subject groups. The multivariate combination of different measures was clearly more powerful and predictive than focusing only on single measures using traditional analysis.

SAMMANFATTNING PÅ SVENSKA

Alzheimers sjukdom (AD) är den vanligaste formen av demenssjukdomar och har blivit ett stort hälso- och samhällsekonomiskt problem. Utmärkande för sjukdomen är förlust av intellektuell kapacitet såsom minne, abstrakt och spatialt tänkande. AD är en progressiv neurodegenerativ sjukdom och antalet personer som insjuknar ökar med åldern. År 2005 var antalet personer i världen med AD beräknat till ca 29,3 miljoner och kostnaden för samhället var ca 315,4 miljarder US dollar [1]. År 2050 beräknas antalet patienter med AD att ha fyrdubblats [2]. Efter att sjukdomsprocessen pågått, sannolikt under många år, förstörs synapser och neuron successivt. Som en följd av detta sker en förminskning av specifika hjärnområden (atrofi av hjärnan). De första områdena som drabbas är de mediala temporalloberna, (entorhinalcortex och hippocampus), så småningom sprids sjukdomsprocessen och därmed atrofin till andra områden i hjärnan**.** Även hjärnans kemi påverkas tidigt och dessa förändringar sker troligtvis innan de strukturella förändringarna har påbörjats. Sjukdomen får tragiska konsekvenser för både patienter och deras familjer. På grund av detta är vi i stort behov av att kunna ställa en tidig diagnos av sjukdomen och finna nya metoder för behandling. I dagsläget finns det inga mediciner mot AD utan bara behandlingar som bromsar sjukdomsförloppet.

Med hjälp av metoder så som magnet resonans ”imaging” (MRI) och magnet resonans spektroskopi (MRS) kan vi i dag studera sjukdomsförloppet. MRI gör det möjligt att visualisera olika områden i hjärnan och med MRS kan man mäta kemiska processer i hjärnan. Nya metoder för analys av MR-data ger oss möjligheten att på ett snabbt och enkelt sätt erhålla stora mängder data. Man har länge fokuserat på att hitta en sjukdomsmarkör för AD, t.ex. en hjärnregion eller ett ämne. På grund av sjukdomens komplexitet så tror vi att en markör inte räcker för att kunna ställa en korrekt diagnos.

Målet med denna avhandling är att kombinera multivariat data analys med MRI och MRS och därigenom kunna monitorera sjukdomsförlopp och behandling. Multivariat data analys kan reducera komplexiteten i de stora mängder data som erhålls från de olika MR-metoderna. På detta sätt kan mönster ses i data vilket i vanliga fall skulle vara svårt att observera med traditionella statistiska metoder.

I denna avhandling ingår fyra arbeten, vilka alla kombinerar en eller flera MR-metoder med multivariat data analys. **Studie I** kombinerar multivariat data analys med MRS för att monitorera behandling med en anti-epileptisk medicin (Carbamazepin) i en musmodell för megencephalit. **Studie II** kombinerar multivariate data analys med MRS för att monitorera behandling med en acetykolin-esteras hämmare (Donepezil) i en musmodell

för AD. **Studie III** är en multi-center studie där MRI data samlats in från sex olika länder i Europa. Data har samlats in från patienter med AD, patienter med tidiga minnesbesvär och friska frivilliga försökspersoner. Multivariat data analys användes för att analysera alla MRI data för att upptäcka skillnader i hjärnans struktur mellan de olika grupperna. **Studie IV** kombinerar både MRI och MRS med multivariat data analys för att särskilja mellan patienter med AD och friska frivilliga försökspersoner. Vi önskade även undersöka värdet av MRS som ett komplement till MRI vid tidig diagnostisering av AD.
Genom att kombinera multivariat data analys med MRI och MRS kan vi visa att det är möjlig att monitorera både behandling och sjukdoms förlopp. Metoderna kan på ett bra sätt appliceras i både djurmodeller och i klinisk praxis. Förändringar i hjärnans kemiska sammansättning kunde observeras efter behandling och atrofimönster i hjärnan kunde identifieras. Dessa metoder har stor potential att i framtiden kunna användas vid tidig diagnostisering och behandling av AD.

LIST OF ABBREVIATIONS

Aβ	β-amyloid
AchEI	Acetylcholinesterase inhibitors
AD	Alzheimer's Disease
ADAS-Cog	Alzheimer's disease assessment scale –cognitive subscale
ADNI	Alzheimer's Disease Neuroimaging Initiative
Ala	Alanine
ADRDA	Alzheimer's Disease and Related Disorders Association
ANIMAL	Automated Non-linear Image Matching and Anatomical Labeling
ApoE	Apolipoprotein E
APP	Amyloid precursor protein
ART	Alzheimer's Research Trust
Asp	Aspartate
CBZ	Carbamazepine
CDR	Clinical dementia rating scale
Cho	Choline
CSF	Cerebrospinal fluid
CTL	Healthy control subject
Cr	Creatine
Ctx	Cortex
CV	Cross validation
DA	Discriminant analysis
DSM IV	Diagnostic and Statistical Manual of Mental Disorders, 4th edition
FID	Free induction decay
GABA	γ-aminobutyric acid
Glu	Glutamate
Gln	Glutamine
GPC	Glycerophosphorylcholine
Hipp	Hippocampus
ICC	Intra class correlation coefficients
ICD 10	International Statistical Classification of Diseases and Related Health Problems, 10th revision
INNOMED	Innovative Medicines in Europe
INSECT	Intensity-Normalized Stereotaxic Environment for Classification of Tissues
IR	Inversion recovery
Lac	Lactate
LR+	Positive likelihood ratio
MCI	Mild cognitive impairment
M-Ins	*Myo*-inositol

MMSE	Mini mental state examination
MP-RAGE	Magnetization-prepared rapid acquisition gradient echo
MRI	Magnetic resonance imaging
MRS	Magnetic resonance spectroscopy
NAA	N-acetyl aspartate
NAAG	N-acetylaspartylglutamate
NFT	Neurofibrillary tangles
NINCDS	National Institute of Neurological and Communicative Disorders and Stroke
NMDA	N-methyl-D-aspartate
NMR	Nuclear magnetic resonance
NP	Neuritic plagues
OPLS	Orthogonal partial least squares to latent structures
PCA	Principal component analysis
PCho	Phosphorylcholine
PCr	Phosphocreatine
PET	Positron emission tomography
PLS	Partial least squares to latent structures
PRESS	Point resolved spectroscopy
RARE	Rapid acquisition with relaxation enhancement
RF	Radio-frequency
ROI	Region of interest
SPM	Statistical Parametric Mapping
Str	Striatum
Tau	Taurine
Tau-p	Hyperphosphorylated tau
VIP	Variable of importance in the projection
VOI	Volume of interest
WHO	World Health Organization

LIST OF PUBLICATIONS

I. **Westman E**, Spenger C, Wahlund L-O, Lavebratt C. Carbamazepine treatment recovered low N-acetylaspartate+N-acetylaspartylglutamate (tNAA) levels in the megencephaly mouse BALB/cByJ-Kv1.1$^{mceph/mceph}$. Neurobiol Dis. 2007 Apr; 26(1):221-8. Epub 2006 Dec 29.

II. **Westman E**, Spenger C, Oberg J, Reyer H, Pahnke J, Wahlund L-O**.** In vivo 1H-magnetic resonance spectroscopy can detect metabolic changes in APP/PS1 mice after donepezil treatment. BMC Neurosci. 2009 Apr 7; 10:33.

III. **Westman E**, Simmons A, Zhang Y, Muehlboeck J-S, Tunnard C, Liu Y, Collins L, Evans A, Mecocci P, Vellas B, Tsolaki M, Kłoszewska I, Soininen H, Lovestone S, Spenger C and Wahlund L-O for the AddNeuroMed consortium. Multivariate analysis of MRI data for Alzheimer's disease, mild cognitive impairment and healthy controls. *Submitted.*

IV. **Westman E**, Wahlund L-O, Foy C, Poppe M, Cooper A, Murphy D, Spenger C, Lovestone S, Simmons A. Combining MRI and MRS to distinguish between Alzheimer's disease and healthy controls. *Submitted.*

TABLE OF CONTENTS

1 INTRODUCTION

AddNeuroMed a part of InnoMed, (Innovative Medicines in Europe) is an Integrated Project funded by the European Union Sixth Framework program [3]. AddNeuroMed develops and validates novel surrogate markers of disease and treatment, based upon in vitro and in vivo models in animals and humans, using Alzheimer's disease (AD) as a testing platform. AD was chosen as a testing platform since dementia has become a great health and socioeconomic problem of modern society. The neuroimaging part of AddNeuroMed uses magnetic resonance imaging (MRI) and magnetic resonance spectroscopy (MRS) to establish imaging markers for early diagnosis and detection of disease and efficacy of disease modifying therapy in man as well as translational imaging biomarkers in animal models of AD.

Alzheimer's disease is one of the most common forms of neurodegenerative disorders. The disease is characterized by a gradual loss of cognitive functions such as episodic memory. The ability to visualize AD pathology in the brain implies great advancement for making diagnosis and evaluation of disease-modifying treatment strategies. MRI is a non-invasive technique, which enables the production of virtual slices through a body and thus the study of the anatomy and pathology in a living subject. MRS has provided useful information on the chemical profile of the living brain in different neurodegenerative diseases, in particular AD. These techniques are widely available and the image acquisition can be reproduced. The methods are sufficiently stable over the required course of time to monitor patients longitudinally. Further, these techniques are tolerated with ease by patients with dementia [4]. Hence, these techniques can be used to study disease progression in vivo. This also provides for the possibility to follow drug effects longitudinally. Moreover, MRI and MRS reflect true translational biomarkers since these techniques are similarly applicable in animal models and in man.

Due to recent advances in magnetic resonance image and spectral analysis, large amounts of data with high complexity and dimensionality can be received. Multivariate data analysis methods such as principal component analysis (PCA) [5], partial least squares to latent structures (PLS) [6, 7] and orthogonal partial least squares to latent structures (OPLS) [8, 9] provide tools to deal with vast amounts of data. These methods reduce the dimensionality (to 2- or 3-dimentions) and complexity. This makes it possible to visualize inherent patterns in the data.

The overall aim of this thesis is to combine magnetic resonance imaging and spectroscopy with multivariate methods to monitor disease and treatment in Alzheimer's disease. A smart combination of different MR measures (patterns of disease) can be a potent biomarker in itself for disease diagnosis, progression and treatment.

2 ALZHEIMER'S DISEASE

Dementia is the third most common cause of death in society today, superseded only by cancer and cardiac vascular disorders, and AD is the most common form. There are other types of dementia such as frontotemporal dementia, dementia with Lewy bodies and secondary dementia. AD is a progressive neurodegenerative disorder and the prevalence increases with age. The estimated cost of the dementia in the world has been calculated to 315.4 billion USD based on an estimated 29.3 million demented patients in 2005 [1]. The number of patients with AD has been predicted to quadruple by the year of 2050 [2].

The early symptoms of the disease are failure in short term memory, learning problems and problems in processing new information. This is followed by speech impairment and general decline in cognitive functions. The patients lose their ability to function in daily life and need increasingly more care as the disease progresses. For the diagnosis of AD, patients need to undergo several evaluations and cognitive tests, and brain imaging techniques are today integrated into the diagnostic battery (especially MRI). To be able to make a definite diagnosis of AD a post-mortem analysis is still necessary.

The pathological hallmarks of AD are degeneration of cholinergic neurons, extracellular deposits of neuritic plaques (NP) constituted mostly of β-amyloid (Aβ) [10, 11] and intracellular neurofibrillary tangles (NFT) formed by hyperphosphorylated tau [12]. Loss of neurons and synapses are other pathological changes connected with AD.

AD can have a late onset and an early onset and the disease can be sporadic or familial. Sporadic AD is mainly age-related, while familial AD is connected to a number of different gene mutations, involved in the production of Aβ. However, not all subjects with late onset have a sporadic form of AD, hereditary factors can be involved as well and not all early onset subjects have a familial form of AD.

Since both the patient and his/her family are affected by the consequences of the disease, there is a great need for new diagnostic tools for early detection with the hope that future medicines and early intervention will stop or significantly reduce disease progression and deterioration. There is also a demand for tools for distinguishing between different types of dementia and for predicting which of the MCI patients that will convert to AD. Unfortunately, there is no cure for AD at present and the drugs that are available mainly reduce symptoms and do not affect the etiology of the disease.

2.1 GENES AND RISK FACTORS

Most AD cases are sporadic but a few cases, less than one percent, are inherited familial forms with known gene mutations. The sporadic form of AD is heterogeneous and multifactorial in its pathogenesis and it is thought to be a combination of genotype and several environmental risk factors. Two well-known risk factors are old age and the ε4 allele of Apolipoprotein E (ApoE, chromosome 19). There are several polymorphisms of ApoE including the different alleles ε2, ε3 and ε4. Carriers of the ε4 allele run an increased risk of developing AD [13]. ApoE is involved in the metabolism and delivery of cholesterol and triglycerides and the ε4 allele is involved in both Aβ deposition and tangle formation. The ApoE ε4 allele has the highest affinity to Aβ, it is associated with senile plaques and is believed to accelerate fibrillogenesis [14].

The familial forms of AD have been shown to be a direct cause of mutations in specific genes. It has also given some insight into the probable etiology of sporadic forms. Associated genes are amyloid precursor protein (APP, chromosome 21) [15], Presenilin 1 (chromosome 14) [16] and Presenilin 2 (chromosome 1) [17]. Increased production and/or deposition of Aβ-peptides and increase in the more aggregating form $A\beta_{1-42}$ [18] are among others the phenotypes coupled to these genotypes.

2.2 NEUROPATHOLOGY

The two major pathological hallmarks of AD are extracellular plaques and intracellular tangles and these were first described by Alois Alzheimer in 1907. Plaques and tangles are built of aggregates of Aβ [10, 11] and hyperphosphorylated tau (tau-p) [12], respectively. Aβ can be found both as intracellular and extracellular and it aggregates into both oligomers and fibrils. The aggregates of tau-p are only found within the neurons [19]. Other characteristics of AD are synaptic loss and neuronal cell death, leading to brain atrophy (decrease in brain volume).

The Aβ peptides are the main protein component of amyloid plaque and cerebrovascular amyloid. Aβ is a product of the sequential proteolytic cleavage of a larger membrane associated glycoprotein, the amyloid precursor protein (APP). APP can be processed in different ways. The two major ways are the amylogenic and the non-amylogenic. The non-amylogenic pathway is processed by α- and γ- secretase and the end product is an Aβ type which cannot form plaque. In contrast, the amylogenic pathway is governed by β-secretase. This enzyme cleaves APP in a way which forms Aβ competent of forming plaque. In plaque, Aβ exits primarily in a fibrillary form, where the predominant species end with the amino acids 40 and 42 ($A\beta_{40}$ and $A\beta_{42}$),

where the latter is more amyloidogenic. The Aβ fibrils have a noncrystalline nature and the peptides have limited solubility. In plaque, Aβ adopts β-Sheet conformation. Diffusible ligands derived from Aβ, including Aβ dimers and trimers have been proven to cause progressive loss of hippocampal synapses and induce neuronal cell death [20]. Most of the neuronal toxicity seen in AD is believed to be a cause of intracellular Aβ oligomers [21, 22]. However, the physiological role of Aβ is not yet fully known [23].

The NFTs consist of intracellular bundles of paired helical filaments of hyperphosphorylated tau proteins, which reduce the ability to bind to microtubules. This leads to cytoskeletal degeneration and cellular death.

The amyloid cascade hypothesis [24] is today the most prominent theory proposed to explain the pathogenesis of AD. This theory states the involvement of the Aβ peptide in driving the neurodegerative process and causing AD. The imbalance between production and clearance of Aβ leads to its accumulation. This imbalance further initiates a series of processes leading to the formation of NP and NFT, synaptic dysfunction, microgliosis and neuronal loss. These pathological changes probably begin many years before the first clinical symptoms are observed.

Braak-stageing [25] is commonly used to define the stage of AD according to the manner in which the neurofibrillary pathology has spread and it distinguishes six stages. During the first two Braak stages the pathology is confined to the entorhinal cortex/transentorhinal cortex with minimal involvement of the hippocampus. In the third and fourth stages the disease has spread to the hippocampus and the medial temporal limbic areas and in the final two stages the pathology has extended to the isocortical association areas. The distribution of Aβ is of limited significance for the differentiation of neuropathological stageing. The plaques are first visible in orbitofrontal and temporal cortices and spread further to parietal cortex and throughout the neocortex.

2.3 CLINICAL DIAGNOSIS

The National Institute of Neurological and Communicative Disorders and Stroke (NINCDS) and the Alzheimer's disease and related Disorders Association (ADRDA) outlined the clinical criteria of AD [26]. The NINCDS–ADRDA describes three levels of certainty for the diagnosis of AD: (I) possible, (II) probable and (III) definite. The criteria for possible AD require that there is a dementia syndrome with an atypical onset, presentation or progression without known etiology. No comorbidity capable of producing dementia is believed to cause the syndromes. For the diagnosis of probable

AD, dementia has been established by neuropsychological examination. Progressive cognitive impairment has to be present in two or more areas of cognition. The onset of the deficits has occurred between the ages of 40-90 years. There must be an absence of other diseases capable of producing dementia. Finally, to make the diagnosis of definite AD, the patient must fulfill all the criteria for probable AD and there must be histopathologic evidence of AD by either autopsy or biopsy. There are also other outlined clinical criteria for AD such as DSM IV (Diagnostic and Statistical Manual of Mental Disorders, 4th edition) published by the American Psychiatric Association and ICD 10 (International Statistical Classification of Diseases and Related Health Problems, 10th revision) by the World Health Organization (WHO).

For the clinical diagnosis of AD, patient evaluation and history is assessed and this is of great importance. There are several other tools used to support in the diagnostic procedure , such as the mini mental state examination (MMSE) [27], the clinical dementia rating scale (CDR) [28] and Alzheimer's disease assessment scale –cognitive subscale (ADAS-Cog) [29]. The MMSE test is a 30-point questionnaire used for measuring severity and decline in cognition. It deals with function, such as memory function, calculation, language abilities and attention. Gaining a score of 24-30 is considered as no dementia, 19-23 as mild dementia and 13-18 indicates moderate dementia. The CDR scale is also used for the evaluation of stageing severity of dementia. This is a five point scale, rating six functional domains. These are memory, orientation, judgment and problem solving, community affairs, home and hobbies and finally personal care. The five point scale is as follows:

CDR=0: no dementia
CDR=0.5: very mild dementia
CDR=1: mild dementia
CDR=2: moderate dementia
CDR=3: severe dementia

ADAS-Cog [29] is a subscale of ADAS, which was designed to measure the severity of the most important symptoms of AD. This subscale is a popular cognitive testing instrument used in clinical trials. This test includes 11 tasks measuring cognitive disturbances, language, attention and other cognitive abilities. Finally, brain scan examinations are performed on routine bases to aid in the clinical evaluation. MRI is today the first choice in many countries.

2.4 BIOMARKERS

In recent years, the understanding of underlying biological functions of AD has advanced. New biomarkers of the disease have been recognized including MRI (early structural changes in the medial temporal lobe, particularly etorhinal cortex and hippocampus), positron emission tomography (PET) (molecular neuroimaging changes) and cerebrospinal fluid (CSF) biomarkers (changes in levels of Aβ, tau proteins and ratios of the two). Since the evidence of the use of these biomarkers is growing, it allows the incorporation of these into the advanced diagnostics of AD. The NINCDS–ADRDA criterion is still the standard for making the diagnosis of AD. Dubois and coworkers have suggested a revision of this criterion. This new criterion is still centered on a clinical core of early and significant episodic memory impairment. It also includes at least one, preferably more than one abnormal biomarker among MRI, PET and CSF [30, 31]. The combination of different biomarkers may prove to be more useful than using single biomarkers separately.

Different disease modifying treatments are emerging from the pipelines of pharmaceutical companies. Robust diagnostic markers are therefore needed to ensure that therapies are targeted at the correct patient population.

2.5 MILD COGNITIVE IMPAIRMENT

Many patients with memory impairment do not necessarily meet the clinical criteria for dementia. The concept of mild cognitive impairment (MCI) is thought to be a transitional phase between being cognitively normal and having an AD diagnosis. Patients with MCI have a higher risk of developing AD than elderly with normal cognitive function[32]. The concept of MCI is rather difficult to describe since it is a very heterogeneous group. The diagnostic accuracy of the criteria today is low to moderate[33]. For this reason it has been divided into different categories, namely amnestic (having memory deficits) and non-amnestic (having no memory deficits, but other cognitive problems). These categories can be further split into single and multiple domains [34]. Single domain means that the subject has one cognitive deficit and multiple domains involve several different cognitive deficits. The common criterion for describing a subject with MCI states that the subject has memory complaints and objective memory impairment but preserved general cognitive functions and handles daily life and is not demented[35]. The clinical group of MCI is very important for both preventive trials and evaluating MR markers for early diagnosis and monitoring of disease progression [34].

2.6 MRI AND MRS IN AD

Translational biomarkers in Alzheimer's disease based on non-invasive *in vivo* methods are highly warranted. Magnetic resonance imaging (volumetric and cortical thickness measures of atrophy) and magnetic resonance spectroscopy (biochemical measurements) are non-invasive and applicable *in vivo* in both humans and experimental animals. These biomarkers are highly warranted to monitor disease progression and treatment. With the different techniques available today it is possible to analyze different aspects of AD pathology. There are also other modalities of MR available, diffusion MRI (microstructural), functional MRI (measures brain function and activation) and MR-perfusion (measures blood flow). The definition of an ideal MR marker is that it has to detect a fundamental feature of AD neuropathology, it has to be diagnostically sensitive and specific (validated through neuropathology) and the results have to be accurate and reproducible [34].

MRI has been widely used for the early detection and diagnosis of AD [4, 36, 37]. Manual hippocampal volumetry is currently the most established biomarker for AD in the field of structural imaging and is often considered to be the golden standard. Many studies have applied this technique successfully [38-46]. These studies have demonstrated high accuracy in distinguishing between AD patients and healthy controls. Also measures of entorhinal cortex have been used to discriminate between subjects with AD and controls [40, 41, 47]. Hippocampal volumes and entorhinal cortex measures have been found to be equally accurate in distinguishing between AD and normally cognitive elderly subjects [34]. The changes observed in hippocampus and entorhinal cortex are consistent with the underlying pathology of AD, but it is not yet clear which structures are most useful for early diagnosis [36]. However, manual delineation is very time consuming and usually not very practical in large population studies and drug trials. For this reason various automated data-driven methods are currently being evaluated to detect regional changes. Examples of methods used are voxel based morphometry (VBM) [48-51], deformation based morphometry (DBM) [52] and measurements of cortical thickness [53-55]. These methods in combination with different multivariate statistical analysis methods [55] and analysis algorithms have the potential to be as useful, or even better than for example manually outlined measures of hippocampus for the early detection of AD. Further, combining different measures of atrophy may prove to be useful in distinguishing between different types of dementia. Hippocampal atrophy is not specific for AD; the structure is also highly atrophied in other disorders such as

frontotemporal dementia and hippocampal sclerosis. For this reason combining different measures will improve the accuracy of the clinical diagnosis.

With MRS, changes in the neurochemical profile can be measured in the brain at the cellular level. In AD, molecular neuropathology is thought to precede structural brain changes by several years. Measuring brain metabolism might be a sensitive early marker. Examples of metabolites measured in the brain are N-acetyl aspartate (NAA), *myo*-inositol (m-Ins), choline (Cho), glutamate (Glu), glutamine (Gln) and taurine (Tau) or the corresponding metabolite creatine (Cr) ratios (NAA/Cr, m-Ins/Cr, Cho/Cr, Glu/Cr, Gln/Cr and Tau/Cr). NAA is decreased in several neurological disorders including AD. This metabolite is mainly located in neuronal bodies, axons and dendrites. It is a marker for neural density and/or function. The reduction of NAA in AD patients indicates neuronal or neuronal component loss. It may also reflect neuronal functional disruption [56]. NAA or NAA/Cr is probably the most widely investigated metabolite in AD and altered levels have consistently been found in several studies. Decreased levels have been found in parietal and occipital cortex [57], gray matter [58, 59], hippocampus [60, 61], and posterior cingulate [62, 63]. Myo-inositol, a large sugar-alcohol with a similar structure as glucose, is one of nine isomers of inositol. The function of this metabolite is not well understood. It may be a requirement for cell growth, as an osmoregulator, as a storage form of glucose, or as a detoxification agent in the brain. Elevated levels of *m*-Ins in AD may be related to glial proliferation and astrocytic activation [34, 57, 62]. Increased levels have been observed in parietal and occipital cortex [57], gray matter [59] and posterior cingulate [62]. Glu and Gln are both amino acids that are present in the brain. Glu is the major excitatory neurotransmitter in the brain involved in learning, memory and cognition. Gln is a precursor and storage form of Glu, much of it being located in astrocytes. Reduced levels of Glu have been reported in the hippocampus and cortex in transgenic AD mice [64] and in the hippocampus in patients with AD [65]. Choline is a precursor of acetylcholine and it is also a product of membranial phosphatidylcholine breakdown [66]. In AD there are losses of cholinergic neurons and it was shown in vitro that levels of free choline and glycerophosphorylcholine are higher in AD brains [67]. Moreover, higher levels of choline may be explained by an increased cell membrane phospholipid turnover in demented brains [68]. Tau is a free amino acid present in the brain. Areas in the brain which contain the highest concentrations of Tau are the dorsal striatum and the hippocampus [69]. Tau may be involved in a number of biological functions. It acts as an organic osmolyte in the brain, involved in cell volume regulation. Another role of

taurine is modulation of the actions of neurotransmitters. Elevated levels of Tau have been reported in AD mice [70].

2.7 TREATMENT

There is, at present, no cure for AD and the drugs are designed to reduce symptoms and do not affect the etiology of the disease. Many treatment strategies have been explored to prevent and slow down the disease, with limited success. One of the major problems is to define targets for the drug treatment and many options have been explored such as symptomatic/neurotransmitters, anti-amyloid treatment and inhibition of tau formation. The anti-amyloid treatments focus on slowing down or reversing the processes that lead to the formation of Aβ in the brain. The treatment strategies, focusing on tau formation attempt to inhibit the kinases causing tau hyperphosphorylation. Today, the only treatments used in clinical praxis are symptomatic cholinergic transmitter therapy with acetylcholinesterase inhibitors (AchEI) (donepezil, rivastigmine and galantamine) and the N-methyl-D-aspartate (NMDA) antagonist, memantine. It has been demonstrated in clinical studies that memantine has beneficial effects on functions of daily life [71] and this drug can safely be given in combination with AchEI [72]. AchE inhibitors, enhance the lifetime of the neurotransmitter acetylcholine in the synapse and thus increase the cholinergic neurotransmission [73]. The three different AchEI mentioned above, all have different pharmacological properties, with diverse selectivity, inhibition and bioavailability [74].

Symptomatically, donepezil improves cognitive functions in AD patients [75, 76]. Using MRS in patients, brain metabolites and neurotransmitters can be non-invasively measured and effects on brain NAA levels caused by donepezil have been reported [76, 77]. Moreover, effects on m-Ins and Cho in the hippocampus of AD patients treated with donepezil have been observed [78]. Significantly, abated decrease in total hippocampus size has also been demonstrated [76]. Effects on the metabolites ratios Tau/Cr and Cho/Cr have also been observed in a transgenic mice model of AD after donepezil treatment [79].

2.8 ANIMAL MODELS IN AD

Different animal models that express one or more mutant proteins associated with AD have been created. They offer the opportunity to study some of the pathological processes of AD *in vivo*. Different animal models that express one or more mutant protein associated with AD allow us to study various features of AD [80-84]. While some

models may express different levels of β-amyloid [85, 86], other models modulate the production of tangles [87, 88]. The APP/PS1 mouse [89, 90] coexpresses the mutated forms of human β-amyloid precursor protein (APP) and mutated human presenilin 1 (PS1) and thus reflects important features of the neurochemical profile in humans [64].

2.9 THE MEGENCEPHALY MICE

The megencephaly mice (BALB/cByJ-*Kv1.1*$^{mceph/mceph}$)[91] display excessive brain growth and complex partial seizure related to a mutation within the potassium channel gene *Kv1.1* producing a malfunctioning protein[92]. *Kv1.1* is expressed in neurons and different subunits form tetramers together, which create channels that regulate neuronal excitability and signaling. The *mceph/mceph* show increased firing frequency following electric pulse trains in hippocampal neurons[92]. The increase in brain size is progressive and primarily affects the hippocampus and ventral cortex[93]. Both more and larger neurons cause the enlargement of the hippocampus[91, 94].

3 MAGNETIC RESONANCE IMAGING AND SPECTROCOPY

Magnetic resonance imaging (MRI) and magnetic resonance spectroscopy (MRS) are two non-invasive methods and they are used to study brain anatomy and the neurochemical profile, respectively. These techniques are based on the interactions between an atomic nucleus with a nuclear spin angular momentum and an external magnetic field. About a third of all naturally occurring isotopes has a spin, and can therefore be used for nuclear magnetic resonance. One of the most commonly used isotopes is the ^{1}H hydrogen atom. The hydrogen atom is found in all biochemicals and has the strongest response of all the atomic nuclei. The phenomenon of nuclear magnetic resonance (NMR) can be described in three steps. These are magnetization, excitation and detection.

3.1 MAGNETIZATION

The spin (I) is an important property of the nucleus. The value of I depends on the atomic weight and the atomic number and it can be either 0, half-integral or integral values. If a nucleus has an I-value of zero it does not interact with an external magnetic field. This means that the nucleus has an even atomic weight and an even atomic number. An odd atomic weight leads to a half-integral value (^{1}H has a spin of ½). Finally an even atomic weight and odd atomic number gives us an integral value of I.
When describing a rotating nucleus, it is easy to picture it as a bar magnet (figure1). The magnetic field of the bar magnet proceeds from south to north, while the magnetic field, caused by the nucleus is oriented in the direction of the axis of rotation.

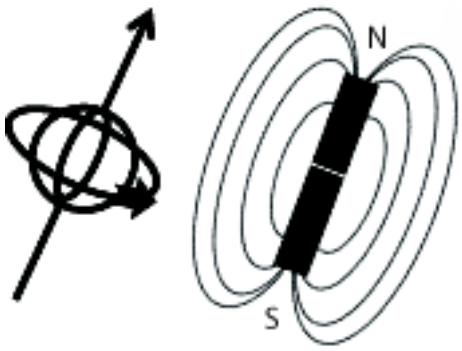

Figure 1. A nucleus compared with a bar magnet

Each nucleus in a sample has a different vector representing its magnetic moment and the direction of the vectors is randomly distributed (figure 2). This results in a net magnetization, M_0, of zero.

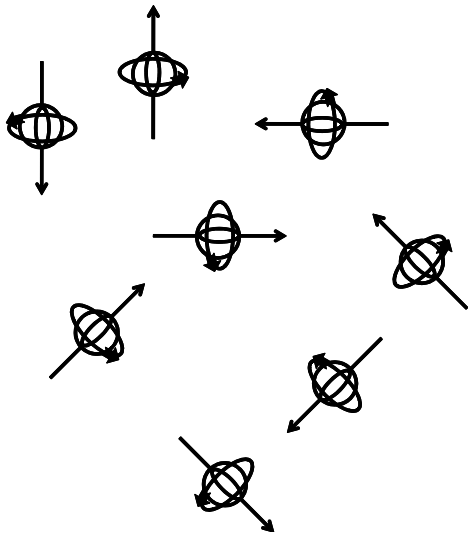

Figure 2. Protons randomly arranged when not exposed to a magnetic field

An external magnetic field, B_0, changes the situation dramatically. Now the protons align along the direction B_0 of the magnetic field (figure 3), rotating in a cone shaped loop around it at a certain angle.

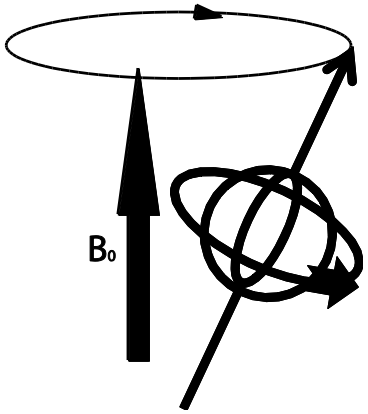

Figure 3. Aligned proton in a magnetic field

This movement is called precession and it occurs as a result of the interaction of the magnetic field and the moving positive charge. The precession speed or the Larmor frequency:

$$\omega_0 = \gamma B_0$$

where B_0 is the field strength in tesla (T) and γ is the gyromagnetic ratio in megahertz (1/(sT)). The value γ is typical for each nucleus, which makes it possible to identify different nuclei from each other.

The spins can be either parallel (low energy level) or anti-parallel (high energy level) to the magnetic field. The number of protons in the lower energy level is greater than the number of that in the higher level (figure 4), leading to a net magnetization that is different from zero. The amount of protons in each level is governed by the Boltzmann´s distribution:

$N_{upper}/N_{lower} = e^{-\Delta E/kT}$ (ΔE is proportional B_0)

where N is the number of protons in the different levels, ΔE is the energy difference between the two levels, T is the temperature in Kelvin (K) and k is Boltzmann´s constant ($1.381 * 10^{-23}$ J K^{-1}). This unequal distribution results in a magnetization with a value of M_0 in the direction of B_0. The direction of the magnetic field has been defined as the z-direction of M_0. The components in the x- and y-direction are zero. If there is absorption of energy more protons will become antialigned, but when the energy supply is stopped, the protons will always strive to return to equilibrium. Larger field strength means a greater value of M_0, resulting in a more intense MR-signal. This induced magnetization is the source of signal for MR-experiments.

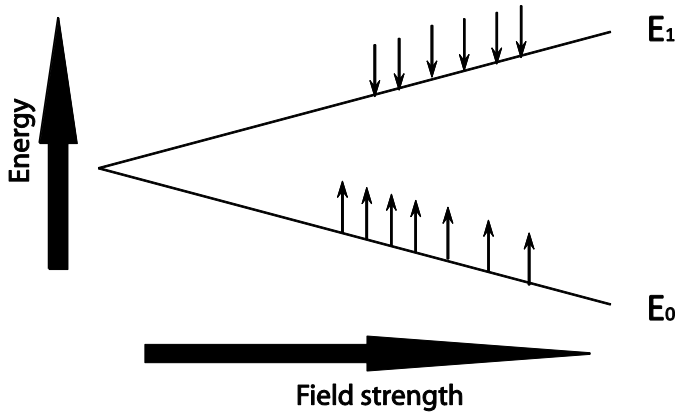

Figure 4. Difference in energy between the two levels

3.2 EXCITATION

To give rise to an MR-signal a radio-frequency (rf) pulse is applied onto the object perpendicularly to the magnetic field B_0, causing another magnetic field B_1 in the y-direction. The rf pulse results in absorption of energy by the protons and a change in direction of the spin vectors. The change in the precession angle of the net

magnetization vector is dependent on the length and amplitude of the rf pulse. In terms of quant physics the absorption of energy will excite protons to the higher energy levels, while protons already in the higher state will release their energy and return to the lower energy level. To make this excitation possible the rf pulse must have the same frequency as the Larmor frequency, i.e. the resonance frequency. This frequency is proportional to the energy difference between the two energy levels.

If an rf pulse is powerful enough to flip the net-magnetization vector M_0 down in the transverse plane, resulting in no net magnetization in the z-direction, the pulse is called a 90 degree pulse. The downward rotation of M_0 down in the transverse plane is orthogonal both to B_0 and B_1. The rf pulse also causes the spin vectors of the protons to synchronize. Before the pulse they basically rotate independently of each other. The system starts to relax back to equilibrium when the rf signal is switched off.

3.3 DETECTION

The protons emit energy when they return back to equilibrium. If a coil is placed orthogonally to the transverse plane, protons will induce a voltage in the coil during precession. Parameters that determine the amplitude and the lapse of time for the induced signal after the rf pulse are the amount of protons in tissue and T_1 and T_2 relaxation times. The signal, which can be detected, is called Free Induction Decay (FID) (figure 5). The FID is the sum of many oscillating waves of differing frequencies, amplitudes and phases. Since the MR-signal is sinusoidal, points are collected at least twice per period. By doing so, the true frequency of a periodic signal can be detected in an economic way.

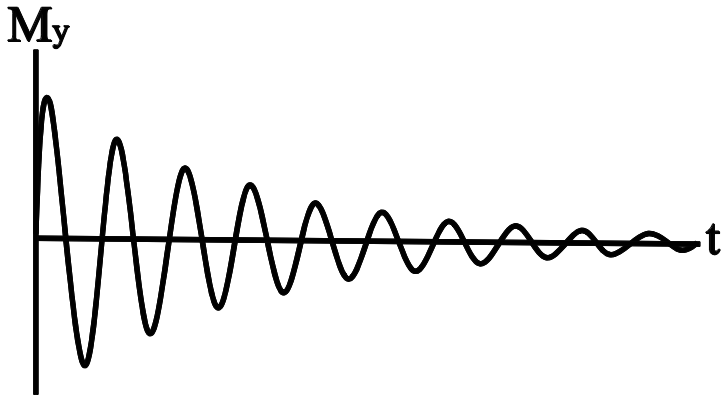

Figure 5. Free Induction decay

3.4 RELAXATION

The relaxation starts both transversely and longitudinally when the radio-frequent field is switched off. The absorbed energy is emitted as radio-frequent radiation. The spins start to dephase and the magnetization in the z-direction returns. Relaxation is the process during which the protons release energy to return to their original configuration. The relaxation is characterized by two relaxation times, T_1 and T_2. Both measure the spontaneous energy transfer by an excited proton. The difference between T_1 and T_2 is the final disposition of the energy. T_2 is always shorter than (or equal to) T_1. This is because the dephasing requires less time than energy emission. T_1 is a time constant, known as the spin-lattice relaxation time or longitudinal relaxation time and it accounts for the time required to get a net magnetization of 63 percent back in the z-direction. It is a measure of how much energy is emitted to the surroundings after a pulse. One way of finding out the value of T_1 is to use a method called inversion recovery (IR), where a 180-degree pulse is applied. M_0 rotates downwards, still parallel to the z-axis, but in the negative direction.

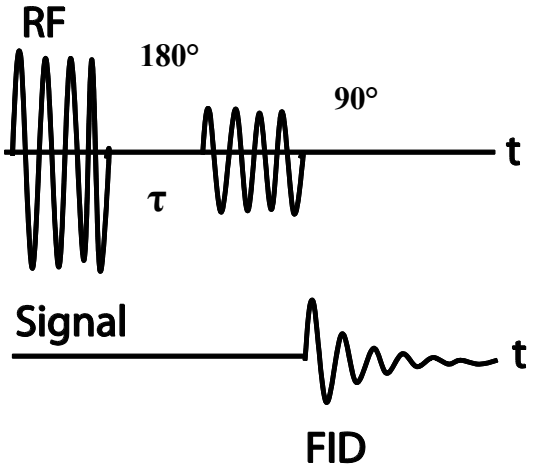

Figure 6. Inversion recovery

No signal is received, since there is no magnetization in the transverse plane. Relaxation starts and after a period of time a new pulse is given, this time a 90-degree pulse (figure 6). This makes the actual magnetization M_z observable in the xy-plane, giving rise to a measurable signal (FID). This process is repeated for different delay times τ. By applying different delay times, the time dependence of M_z can be plotted (figure 7).

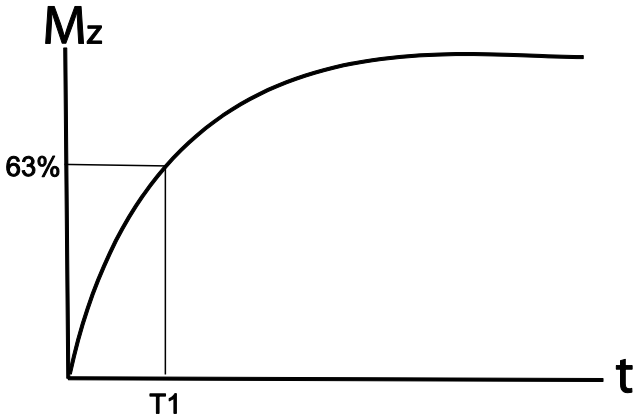

Figure 7. T_1 curve

T_2 is called the spin-spin relaxation or the transverse relaxation. It is the time period required for the transverse component to dephase to 37 percent of its original value. Note that T_2 is the time sequence for the decay of M in the transverse plane, while T_1 is the time sequence for a regrowth of M in the z-direction. Spin-spin relaxation depends on the effect of nuclei precession affecting neighboring nuclei, changing their speed of rotation. The spin echo sequence (figure 8) is a good way of measuring T_2. First a 90-degree pulse flips M_0 down in the transverse plane. During the dephasing some of the spins move faster, leaving other spins behind. Then a second pulse, a 180-degree pulse flips the spins around in the transverse plane. This results in a change of direction of all the spins, leaving the fast spins behind the slow spins. The fast spins catch up with the slow spins resulting in a rephasing. This causes a spin echo of which the amplitude can be measured. Repeating several 180-degree pulses, the decrease in signal strength can be measured and the exponential decay of transverse magnetization can be plotted against time (figure 9).

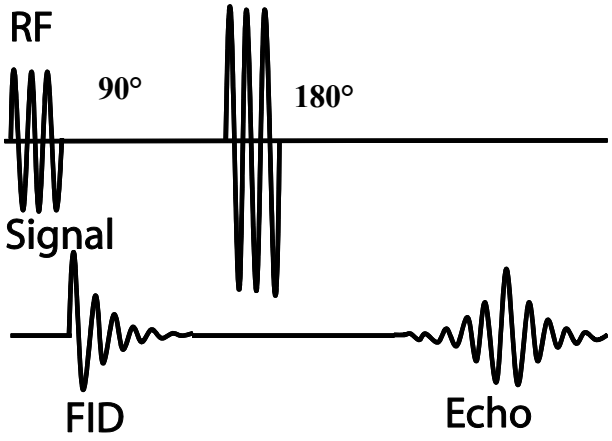

Figure 8. Spin Echo

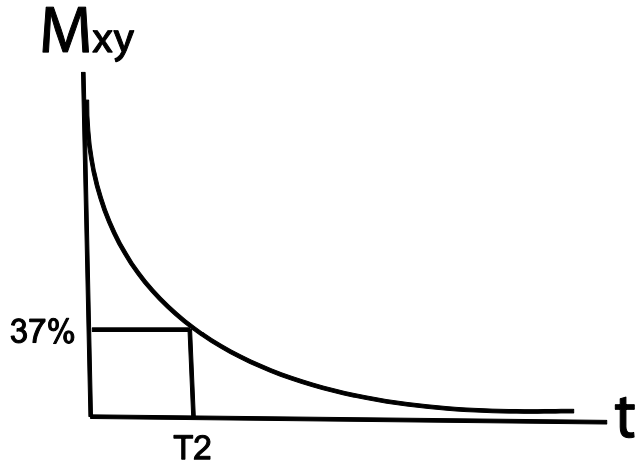

Figure 9. T_2 curve

The calculated T_2 value relies on a perfect magnetic field with no inhomogeneity. However, there is no perfect field due to three different sources of nonuniformity of B_0. These three sources are main field inhomogeneity (M), sample-induced inhomogeneity (MS) and finally gradients. To achieve the total transverse relaxation T_2* the first two sources have to be considered while proper design of the pulse sequence can eliminate the gradient problems.

$1/ T_2^* = 1/ T_2 + 1/ T_{2M} + T_{2MS}$

Main field and sample induced inhomogeneity need to be considered in the formula.

3.5 FOURIER TRANSFORM

The detection of the signal is done in the time domain and not in the frequency domain. The reason is that detection of signal in the frequency domain would require a separate measurement for each frequency, which is time-consuming. In the time domain the whole spectrum can be measured at once. Another reason why measurement in the time domain is preferred is that this makes multidimensional methods available through manipulation of the spin pulses. The pulse measured represents a whole set of frequencies. Hence, the FID has to be Fourier transformed to find out which frequencies are contained.

The signal: $f(t) = \exp(i\delta t) = \cos(\delta t) + i\sin(\delta t)$

The Fourier transform:

$g(\omega)$: The spectrum.

The value of the transform at a particular frequency ω

$$g(\omega) = F(f(t)) = \int_{-\infty}^{\infty} f(t)\exp(-i\omega t)dt$$

There is no signal before the data acquisition starts (t = 0).

In NMR: $g(\omega) = F(f(t)) = \int_{0}^{\infty} f(t)\exp(-i\omega t)dt$

3.6 INSTRUMENTATION

The equipment necessary to perform a MR-experiment includes the following principal components

1. A magnet to create a main magnetic field
2. A gradient system for spatial resolution
3. A transceiver, i.e. an rf-pulse transmitter and an rf receiver
4. A data acquisition system including a computer
5. Power supplies
6. Cooling systems

3.7 MRI ANALYSIS

Two highly automated structural MRI image processing pipelines and manual segmentation were utilized for image data analysis. The first pipeline was developed at the Montreal Neurological Institute and the second pipeline by Fischl and Dale.

3.7.1 Montreal Neurological Institute pipeline

The first pipeline consisted of image intensity non-uniformity correction, segmentation of brain tissue and regional brain parcellation. Initially, data was corrected for intensity non-uniformity using the N3 algorithm [95]. This is a fully automated technique which maximizes the entropy of the intensity histogram and can be applied to any pulse sequence, field strength or MR scanner. The images were subsequently segmented into gray matter, white matter, CSF and lesion subtype using an artificial neural network

classifier termed INSECT (Intensity-Normalized Stereotaxic Environment for Classification of Tissues) (figure 10) [96, 97]. Regional parcellation of the brain was then achieved using the multi-scale analysis ANIMAL technique (Automated Non-linear Image Matching and Anatomical Labeling) (figure 10) which deforms the T1-weighted MP-RAGE volume to match a previously labeled MRI volume. Anatomical labels are defined in the new volume by interpolation from the original labels, via a 3D deformation field [98, 99]. All volumetric measures from each subject were normalized by the subject's intracranial volume.

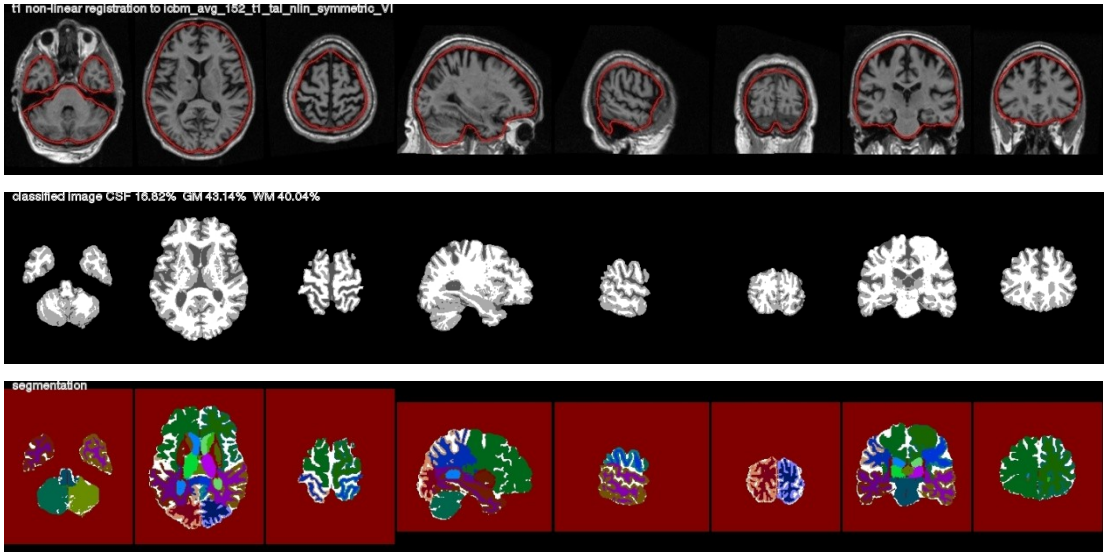

Figure 10. Original images, tissues classification (INSECT) and regional segmentation (ANIMAL)

3.7.2 Fischl and Dale pipeline

The second pipeline, developed by Fischl and Dale produced regional cortical thickness and volumetric measures. Cortical reconstruction and volumetric segmentation includes removal of non-brain tissue using a hybrid watershed/surface deformation procedure [100], automated Talairach transformation, segmentation of the subcortical white matter and deep gray matter volumetric structures (including hippocampus, amygdala, caudate, putamen, ventricles) [100-102] , intensity normalization [95], tessellation of the gray and white matter boundary, automated topology correction [103, 104], and surface deformation following intensity gradients to optimally place the gray/white and gray/cerebrospinal fluid borders at the location where the greatest shift in intensity defines the transition to the other tissue class [105-107]. Once the cortical models are complete, a number of deformable procedures can be performed for further data processing and analysis including surface inflation [108], registration to a spherical atlas

which utilized individual cortical folding patterns to match cortical geometry across subjects [109], and parcellation of the cerebral cortex into units based on gyral and sulcal structure [110, 111]. All volumetric measures from each subject were normalized by the subjects' intra cranial volume.

3.7.3 Manual segmentation of hippocampus

Manual measurements of hippocampal volume were performed on a HERMES workstation (Nuclear Diagnostics, Stockholm, Sweden). Each measurement was performed with constant parameters by a neuroradiologist who was blinded to clinical information. A region of interest (ROI) tool was used within the HERMES multimodality software package, to manually delineate the hippocampal formation using previously defined anatomical landmarks[112]. Intra-rater reliability of the measurements was tested in 15 randomly selected subjects by repeated measurements with an interval of one month. The intra class correlation coefficients (ICC) of the measurements were > 0.93. All measures from each subject were normalized by the subjects' intracranial volume.

3.8 MRS ANALYSIS

All studies involving MRS used the software package LCModel (http://www.s-provencher.com) [113, 114] for the analysis of the spectra. The LCModel algorithm applies linear combinations to calculate the best fit of the experimental spectra to the model spectra. The model spectra are simulated to match the magnetic field strength, type of sequence and sequence parameters used for the data acquisition. The analysis is performed in the frequency domain with raw data (free induction decay (FID)) as the input. In all studies metabolite ratios are used. The ratios are given relative to creatine + phosphocreatine (Cr+PCr) as applied by others [115, 116]. The following 16 metabolites were included in the basis set: alanine (Ala), aspartate (Asp), creatine (Cr), γ-aminobutyric acid (GABA), glucose (Glc), glutamate (Glu), glutamine (Gln), glycerophosphorylcholine (GPC), phosphorylcholine (PCho), *myo*-inositol (m-Ins), lactate (Lac), N-acetylaspartate (NAA), N-acetylaspartylglutamate (NAAG), phosphocreatine (PCr), *scyllo*-inositol, taurine (Tau). Also included are nine simulated macromolecules and lipids. When a metabolite is mentioned in the result section of this thesis, it always implies the corresponding metabolite ratio. Additionally, the metabolites NAA and Cho in the result section refer to the sums NAA= NAA+NAAG and Cho= GPC+PCho.

To ensure that differences in tissue composition did not account for metabolic differences between subject groups (study IV), we segmented the 3-dimensional inversion recovery prepared spoiled GRASS dataset using SPM (Statistical Parametric Mapping) software (http://www.fil.ion.bpmf.ac.uk/spm) to determine the percentage of gray and white matter and CSF composition within each MRS voxel. The metabolite concentrations reported by LCModel were divided by the fractional content of brain tissue (p[GM] + p[WM], where p[GM] and p[WM] represent the percentage of gray matter and white matter in the voxel, respectively) to adjust for the relative proportion of cerebrospinal fluid (CSF) in the MRS voxel.

4 MULTIVARIATE DATA ANALYSIS

The following sections are a short background and an overview of the multivariate methods used. Multivariate analysis performed in the thesis has been done using the software package SIMCA (Umetrics AB, Umea, Sweden).

4.1 PREPROCESSING

Preprocessing is a very important step in building an adequate model and has to be performed in a correct manner. There are many ways in which pre-processing can be done. This section will only describe the methods used in the studies included in this thesis. All analyses were performed using mean centering and unit variance scaling. Mean centering improves the interpretability of the data, by subtracting the variable average from the data. By doing so the data set is repositioned around the origin. Large variance variables are more likely to be expressed in modeling than low variance variables. Consequently, unit variance scaling was selected to scale the data appropriately. This scaling method calculates the standard deviation of each variable. The inverse standard deviation is used as a scaling weight for each MR-measure.

4.2 PCA

The basis of multivariate data analysis is principal component analysis (PCA) [5] and it is an unsupervised method, which means that it does not use *priori* information about groups for the analysis. The representation of a multivariate data table X consisting of rows (observations) and columns (variables) as a low-dimensional plane, is an important feature of PCA. Statistically, PCA reduces the dimensionality and complexity of the data by finding lines and planes in the K-dimensional space (K=number of variables in the model) that approximates the data in the best way possible in the least squares sense. This gives us the opportunity to get an overview of the data to observe group belonging, trends and outliers. It is also possible to view relationships between the observations and the variables. A model usually reduces the K-dimensional space to 2-5 dimensions. The data table X is modeled by PCA in the following way.

$$X = 1 * \bar{x}' + T * P' + E$$

The term $1 * \bar{x}'$ originates from the preprocessing step and represents the variable average. The second term T*P is the matrix product and it models the structure. The

last and final term E is the residual matrix which contains the noise (data not modeled) [117]. PCA matrix representation is shown in figure 11.

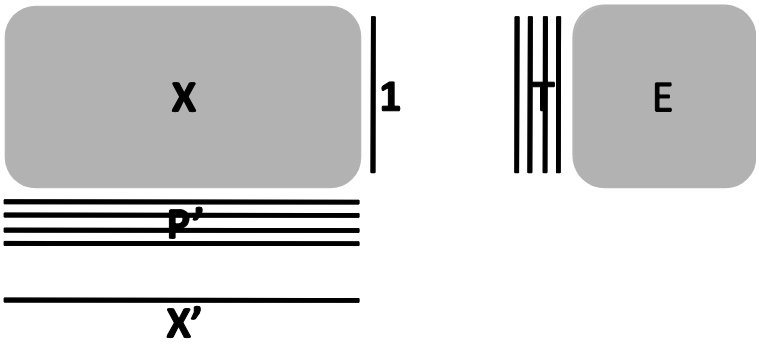

Figure 11. PCA matrix representation

4.3 PLS AND OPLS

Both partial least squares to latent structures (PLS) [6, 7] and orthogonal least squares to latent structures (OPLS) [8, 9] are supervised multivariate data analysis methods. Supervised methods use additional information (dependent variables), directly correlating the independent variables (image or spectral data) with the dependent variables (*priori* information about groups). The methods are similar to PCA in that the independent variables are projected into new coordinate systems. The major difference is that the supervised methods do not attempt to explain as much variance in the original data as possible. Instead they try to maximize the covariance between the dependent and the independent variables. This is done via an inner relationship between the latent variables where the variation of the two sets of variables is described. These methods perform better than PCA when it comes to differentiating between groups.

One way of describing PLS modeling (relationship between two blocks of variables) is that it fits two PCA-like models and aligns them simultaneously, one PCA-like model for X (independent variables) and one for Y (dependent variables). The aims are to model X and Y and to predict Y from X.

$$X = 1 * \overline{x}' + T * P' + E$$

$$Y = 1 * \overline{y}' + U * C' + F$$

The terms $1 * \overline{x}'$ and $1 * \overline{y}'$ originate from the preprocessing step and represent the variable averages. Matrices T and U are information related to the observations. The X-loading matrix P' and the Y-weight matrix C' contain information connected to the

variables. The last and final terms E and F are the residual matrices which contain the noise (data not modeled) [117].

The advantage of OPLS compared to PLS is that the model created to compare groups is rotated. This means that the information related to class separation is found in the first component of the model, the predictive component. The other orthogonal components in the model, if any, correlate to variation in the data not connected to class separation. Focusing the information related to class separation on the first component makes data interpretation easier [9].

The results from the methods are visualized by plotting two or three components in a so-called scatter plot (Figure 12). Components are vectors in the multivariate space along which groups can be separated. These vectors are linear combinations of partial vectors and are dominated by the input variables (x). All the components created by the models are, by definition, orthogonal to each other and span the projection plane of the points. Each point in the scatter plot represents one individual subject. Each component receives a $Q^2(Y)$ value that describes its statistical significance. $Q^2(Y)$ values > 0 are regarded as statistically significant if the model contains more than 100 observations. If the model contains less than 100 observation $Q^2(Y)$ values > 0.05 are regarded as statistically significant. $Q^2(Y)$ is the fraction of the total variation of the Ys (expected class values) that can be predicted by a component according to cross validation (CV).

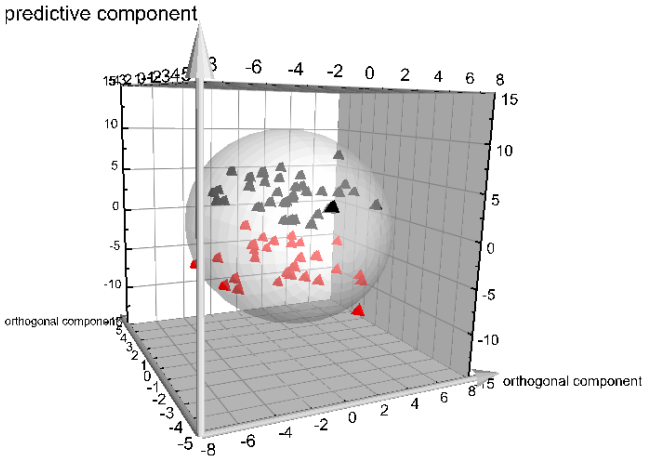

Figure 12. OPLS 3D-scatter plot illustrating the separation between two groups

In the scatter plots differences, if any, between groups can be observed. These differences are based on the input variables. The input variables can be plotted according to their importance for the separation of the groups. All the variables receive a VIP (variable of importance in the projection) value, which reflects its impact in

explaining the group differences. VIP values larger than 1 suggest that the variable is over average involved in the separation of groups (used for PLS modelling). The VIP plots take all the components in the model into account. This makes them unsuitable for OPLS modeling, since all the information related to class separation is found in the first component. For OPLS modeling, we use so-called loading plots which show the variables and their corresponding jack-knifed confidence intervals. Jack-knifing is used to estimate the bias and standard error. Variables with confidence intervals that include zero have low reliability [9]. Covariance is plotted on the y-axis. A variable with high covariance is more likely to have an impact on group separation than a variable with low covariance. Variables below zero in the plot are decreased in the model, while variables above zero are increased.

4.4 CROSS VALIDATION

Cross-validation (CV) is a statistical method for validating a predictive model which involves building a number of parallel models. These models differ from each other by leaving out a portion of the data set each time. The data of the omitted subject is then predicted by the respective model. Leave-one-out cross validation means that one individual subject is left out and the number of parallel models created is the same as the number of observations. CV minimizes the inflation in sensitivity and specificity which is connected to the use of the entire data set as a trainer of the classifier. Failure to cross-validate can result in over-optimistic classification accuracy [55]. There are many ways in which CV can be done and different ways of performing it can give slightly different results [9]. The optimal way to validate a model is of course to have an external test data set. Unfortunately, the number of subjects included in a study limits the use of external test sets.

5 AIM OF THESIS

The general aim of this thesis is to study the applicability of magnetic resonance imaging and magnetic resonance spectroscopy combined with multivariate data analysis to monitor disease and treatment effects in Alzheimer's disease. Can patterns of the disease be used as biomarkers for early diagnosis of the disease and to monitor treatment effects? The methods were applied in both animal models and in man.

The specific objectives were:

- To study alterations in the neurochemical profile in a mouse model for megencephaly (BALB/cByJ-*Kv1.1*$^{mceph/mceph}$) compared to wild type mice and to study the effects of the anticonvulsant drug carbamazepine. This was performed to investigate the potential use of combining *in vivo* MRS and multivariate data analysis to monitor disease and treatment effects.

- To monitor treatment effects of the acetylcholine-esterase inhibitor donepezil in a mouse model of Alzheimer's disease (APP/PS1). This was performed to investigate the potential use of combining *in vivo* MRS and multivariate data analysis to monitor effects of treatment.

- To investigate the potential use of combining different MRI measures (global and regional volumes and cortical thickness measures) with multivariate data analysis in a cross-sectional study to distinguish between patients with Alzheimer's disease, patients with mild cognitive impairment and healthy controls.

- To explore the prospective value of MRS as a complement to MRI in making the early diagnosis of Alzheimer's disease using multivariate data analysis in a cross-sectional study.

6 SUBJECTS AND METHODS

Studies I-III are part of the AddNeuroMed study [3] and the subjects in study IV are derived from the Alzheimer's Research Trust (ART) cohort study [118]. Studies I and II were carried out at the Experimental MR research center at Karolinska Institutet, Solna, Sweden. MRI examinations were performed using a 4.7 T magnet with a horizontal bore (Bruker Biospec Avance 47/40, Bruker, Karlsruhe, Germany) equipped with a 12 cm inner diameter self-shielded gradient system (max. gradient strength 200mTm^{-1}). A commercially available volume coil (Bruker, Karlsruhe, Germany) with an inner diameter of 25 mm was used for excitation and signal detection. Study III is a multi-centre MRI study for longitudinal assessment in Alzheimer's disease. The study is similar to a faux clinical trial and has been established to assess longitudinal MRI changes in AD, MCI and CTL using an image acquisition protocol compatible with Alzheimer's Disease Neuroimaging Initiative (ADNI) [119]. Data was collected at baseline, 3 months and 12 months. However, the data presented here are only from baseline. The approach consists of a harmonized MRI acquisition protocol across centers, rigorous quality control at both the sites and the central data analysis hub and an automated image analysis pipeline. Comprehensive quality control measures have been established throughout the study. An intelligent web-accessible database contains details of both the raw images and the data processed using a sophisticated image analysis pipeline. Data is collected from six different sites across Europe.

- University of Kuopio, Finland
- University of Perugia, Italy
- Aristotle University of Thessaloniki, Greece
- King's College London, United Kingdom
- University of Lodz, Poland
- University of Toulouse, France

Karolinska Institutet was the data coordination center and MR data was sent either electronically or by CD. Data acquisition took place using six different 1.5T MR systems (4 General Electric, 1 Siemens and 1 Picker). At each site a quadrature birdcage coil was used for RF transmission and reception. The population in study IV was derived from a largely community-based population of subjects with AD and elderly people (the ART cohort study). Subjects were scanned using a 1.5 Tesla, GE

NV/i Signa MR-system (General Electric, Milwaukee, WI, USA) at the Maudsley Hospital, London.

6.1 STUDY I

A total of 29 mice were used in this study (Table 1). Carbamazepine was incorporated into R70 pellets (daily intake of 0.5 g) and given orally. The volume of interest for spectroscopy was localized using spin echo sequences with rapid acquisition with relaxation enhancement (RARE) imaging. Spectra were acquired using the PRESS pulse sequence and the voxel was placed in the dorsal hippocampus. LCModel was used for spectral quantification and multivariate data analysis (PLS-DA) was applied to detect group differences.

Table 1. Mouse groups

Mouse type	n	Treatment
mceph/mceph	6	-
mceph/mceph	6	Carbamazepine
wt	8	-
wt	9	Carbamazepine

wt=wild type mice

6.2 STUDY II

A total of 43 female mice were used in this study (Table 2). Donepezil was given i.p. daily for four weeks (0.6mg/kg). Volumes of interest for spectroscopy were localized using spin echo sequences with rapid acquisition with relaxation enhancement (RARE) imaging. Spectra were acquired using the PRESS pulse sequence and voxels were placed in the parietal cortex/hippocampus and striatum. LCModel was used for spectral quantification and multivariate data analysis (PLS-DA) was applied to detect group differences.

Table 2. Mouse groups

Mouse type	N	Treatment
APP/PS1	11	Donepezil
APP/PS1	12	NaCl
wt	10	Donepezil
wt	10	NaCl

wt=wild type mice

6.3 STUDY III

A total of 345 subjects were included in this study. For demographics of the subject cohort see Table 3.

Table 3. Demographics

	AD	MCI	CONTROL
Number	117	118	110
Gender (female/male)	77/43	61/57	60/50
Age	75±6	74±6	73± 7
MMSE	21±5[a]	27±3	29±1
ADAS-Cog[b]	24±10	-	-
CDR	1.2±0.5	0.5	0
Years of education	8±3	9±4	11±5

Data are represented as mean ± standard deviation. AD = Alzheimer's Disease, MCI = Mild Cognitive Impairment, MMSE = Mini Mental State Examination, ADAS-Cog = Alzheimer's Disease Assessment Scale – Cognition, CDR = Clinical Dementia Rating, [a] Number of AD subjects with CDR 0.5= 12, CDR 1=79, CDR 2=26, [b] Data available for AD only.

Following a three plane localizer, a high resolution sagittal 3D MP-RAGE dataset was acquired. Finally an axial proton density / T2-weighted dual echo fast spin echo dataset was acquired. Full brain and skull coverage was required for both of the latter datasets. Automated regional segmentation, cortical thickness measures and manual outlining of hippocampus were performed for each image. Altogether this yielded 75 different volumetric and cortical thickness measures which were used in multivariate data analysis (OPLS).

6.4 STUDY IV

A total of 66 subjects were included in this study. For demographics of the subject cohort see Table 4. T1-weighted images were obtained in the axial plane from each subject. Automated regional segmentation and cortical thickness measures were performed for all the images. Magnetic resonance spectroscopy was acquired from the hippocampus using a PRESS pulse sequence. LCModel was used for metabolic quantification. Altogether, this yielded 69 different volumetric, cortical thickness and metabolite ratio variables which were used in multivariate data analysis (OPLS).

Table 4. Demographics		
Variable	**AD**	**CONTROL**
Number	30	36
Gender (female/male)	15/15	22/14
Age	77±5	77±5
MMSE	23±4	29±1
Years of education	11±3	12±3

Data are represented as average ± standard deviation. AD = Alzheimer's Disease, CONTROL = healthy controls and MMSE = Mini Mental State Examination

7 RESULTS AND DISCUSSION

As previously stated, the aim of this thesis was to test the potential use of combining multivariate data analysis with different magnetic resonance measures to monitor disease and treatment in Alzheimer's disease.

7.1 TREATMENT IN ANIMAL MODELS

We wanted to investigate whether or not it was possible to use the combination of multivariate analysis and MRS to monitor the effects of treatment. A previous study has shown that Carbamazepine (CBZ, an anticonvulsant drug used for the treatment of epilepsy) treatment prevents brain overgrowth in megencephaly mice (BALB/cByJ-*Kv1.1*$^{mceph/mceph}$)[91] and normalizes the expression of trophic molecules [120]. Changes in the neurochemical profile are likely to occur before morphological changes. For this reason we chose to start by investigating the potential use of multivariate analysis and MRS in this mouse model (study I), before moving on to a mouse model for AD (study II).

7.1.1 Study I

We applied MRS to pinpoint differences in the hippocampus between *mceph/mceph* and wt mice. The second aim was to investigate effects of durable oral CBZ treatment on the MR spectra. Using multivariate data analysis, including all measurable metabolites in the PLS-DA model, we could observe significant separations between *mceph/mceph* and wt mice (Q^2=0.787). The most important metabolites for the separation between *mceph/mceph* mice and wt mice were NAA and Cho. *Mceph/mceph* had lower levels of NAA (p=0.001) and Cho (p=0.04) compared to wt mice. Glutamate, glutamine, taurine and *myo*-inositol levels were similar in wt mice and *mceph/mceph* mice showing the specificity of the findings. NAA is considered to be a marker for neural density and/or function. It is likely that in this case the low levels of NAA in *mceph/mceph* mice reflect neuronal dysfunction since hyperexitability of mossy cells, abnormal expression of trophic factors and seizure-like activity have been observed[92-94]. Lower levels of NAA have also been observed in the hippocampus and cortex of patients with epilepsy[121-124] and in idiopathic megalencephaly[125]. The reduced levels of Cho may reflect changes in choline requirements, trafficking or metabolism. There was also a significant separation between *mceph/mceph* mice and *mceph/mceph* mice treated with CBZ (Q^2=0.792). The most important metabolites for the separation

between the two groups were NAA and Gln. NAA levels were significantly higher in treated mice (P=0.03), while Gln did not reach statistical significance using traditional statistical methods (t-test). The treatment recovered both Cho and NAA levels. The Cho levels were fully recovered, while those of NAA were not (p=0.04) compared to those of wt mice. CBZ prevents brain overgrowth and normalizes the abnormal levels of trophic molecules, but the NAA levels are only partly normalized. The reason for this is probably that CBZ has a dampening effect on both the severity and the duration of seizures, but the drug does not eliminate severe seizures. Nevertheless, this further highlights that NAA is a marker for neuronal dysfunction. Creating a PLS-DA model containing all animals (*mceph/mceph,* treated *mceph/mceph* and wt mice) it can be readily observed that the treatment does have an effect (Figure 13).

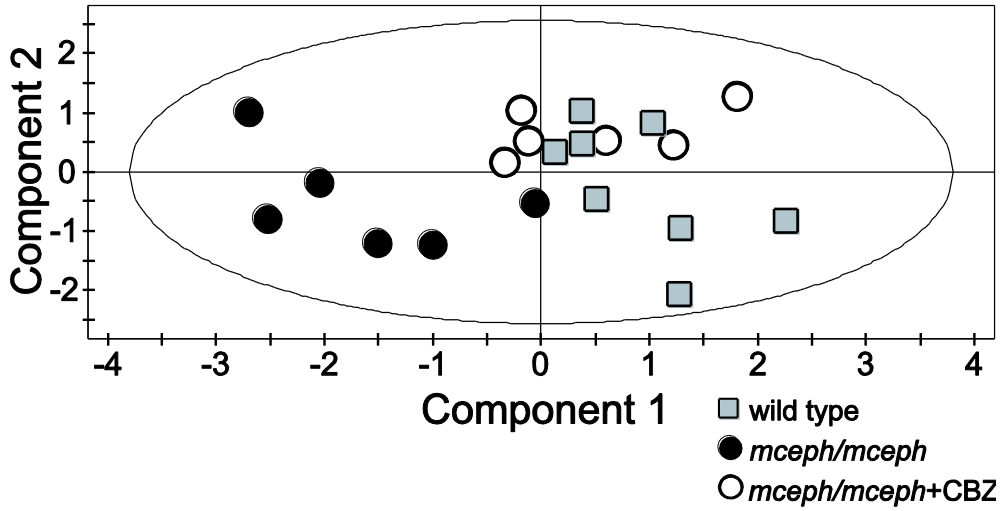

Figure 13. Scatter plot illustrating the normalization of carbamazepine treated *mceph/mceph* mice compared to wild type mice

There were also a significant separation between non-treated and treated wt mice (Q^2=0.150). The most important metabolites for the separation were Cho and m-Ins. Neither of the two metabolites reached statistical significance when tested. However, this shows the strength of multivariate data analysis compared to traditional statistical methods like the t-test. A t-test does not consider correlation patterns in the data and their significance is in many cases destroyed by multiple comparisons.

Distinct differences in MRS spectra between *mceph/mceph* mice and wt mice were depicted and treatment effects of CBZ were monitored using MRS in combination with multivariate data analysis, which demonstrates the potential applications of the techniques .

7.1.2 Study II

Study I demonstrated the potential applications of combining MRS with multivariate data analysis to monitor treatment effects in the *mceph/mceph* mouse model. As a continuation we wanted to investigate if we could apply the same methods to detect treatment effects in an early stage of the development of APP/PS1 mice. The APP/PS1 mouse coexpresses the mutated forms of human β-amyloid precursor protein and mutated human presenilin 1. Consequently, the APP/PS1 mouse model reflects important features of the neurochemical profile in humans suffering from AD. The aim of this study was to investigate if multivariate data analysis could detect changes in the pattern of the metabolic profile after donepezil treatment (an AchE inhibitor). Donepezil was selected as a test candidate, since it is well-known for improving cognitive functions in AD patients[75, 76]. Effects on the brain metabolites N-acetyl-L-aspartate, choline and *myo*-inositol levels have been reported in clinical studies using this drug[76-78].

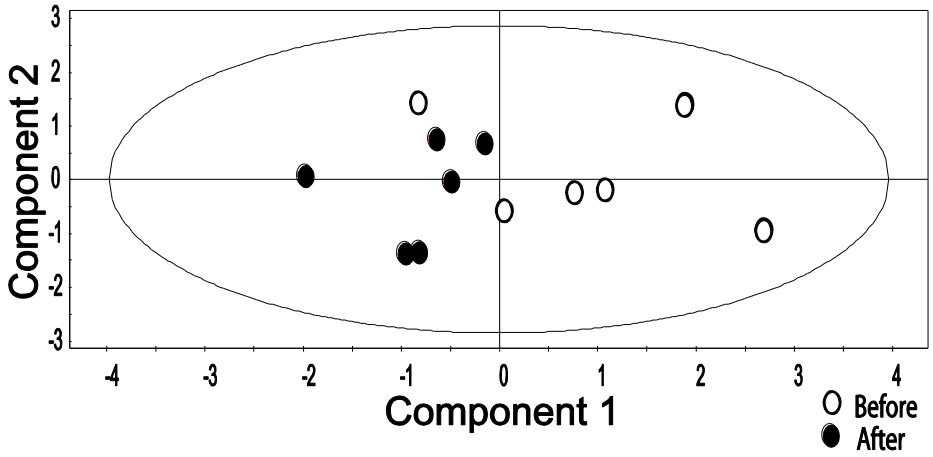

Figure 14. Scatter plot illustrating a significant separation between before and after donepezil treatment in cortex/hippocampus of APP/PS1 mice

Significant differences were observed in the metabolic pattern of APP/PS1 mice in both the striatum (str) and the cortex/hippocampus (ctx/hipp) (Figure 14) before and after donepezil treatment using multivariate data analysis (str: Q^2=0.39, ctx/hipp Q^2=017.), evidencing a significant treatment effect. A significant decrease in the metabolite Tau was related to donepezil treatment in APP/PS1 mice in both brain regions (str: p=0.027, ctx/hipp: p=0.019). It is possible that the decrease in Tau is directly connected to the cholinergic activity since it has previously been shown that Tau inhibits the release of acetylcholine[126]. Lower levels of Tau suggest a reduced inhibitory tone, leading to

increased cholinergic activity. Furthermore, a significant influence on the Cho level was observed in treated APP/PS1 mice compared to untreated animals in str ($p=0.011$). The levels of Cho in str were increased in both untreated and treated APP/PS1 mice, but the increase was partially mitigated by the treatment. These results are in line with AD patient data where increased levels of Cho have been observed[56, 62, 68, 127], as well as a decrease in the levels of this metabolite following donepezil treatment in AD patients[78]. Finally, a treatment effect was also seen in wt mice in str utilizing multivariate data analysis ($Q^2=0.24$) and Glu was significantly increased ($p=0.035$). This increase caused by donepezil treatment could be connected to an increase in cholinergic activity. It is also possible that the glutamate increase is directly connected to donepezil treatment. This increase is somewhat unexpected and needs to be further investigated.

One limitation of this study is that the wt mice were normal C57Bl6 and not the wild type littermates which makes the comparison between the two groups difficult (wt vs. APP/PS1). However, the results do show that it is possible to monitor treatment effects using the combination of multivariate data analysis and MRS which was one of the main aims of the study. Nevertheless, the conclusions drawn connected to human studies should always be interpreted with caution. To make this study more compatible with human studies the experiments have to be performed on older mice. Larger numbers of APP/PS1 mice are required, including wild type littermates. Monitoring the effects of treatment during different stages of life in this mouse model could reveal more detailed information about the effects of this drug.

Multivariate data analysis can detect changes in the metabolic profile in APP/PS1 mice after donepezil treatment. Hence, MR spectroscopy paired with multivariate data analysis may be tested as a tool in drug testing and evaluating drug effects in other settings, especially clinical trials. Effects on several metabolites that are measurable *in vivo* using MR spectroscopy were observed. Changes in Tau and Cho could possibly be related to changed cholinergic activity caused by donepezil treatment.

7.2 MONITOR DISEASE IN PATIENTS

We have now demonstrated that the combination of MRS and multivariate data analysis can be used for monitoring disease and treatment effects in different mouse models. The methods seem powerful and robust and ready to be tested in patient data sets.

7.2.1 Study III

The aim of this study was to investigate if we could discriminate between Alzheimer's disease (AD), mild cognitive impairment (MCI) and elderly control subjects using multivariate data analysis (OPLS) in combination with different MRI measures (regional cortical volumes, regional cortical thickness measures and manual hippocampal measures). We wanted to investigate how these different measures performed using them separately and pooled together in multivariate models for discriminating between the different groups.

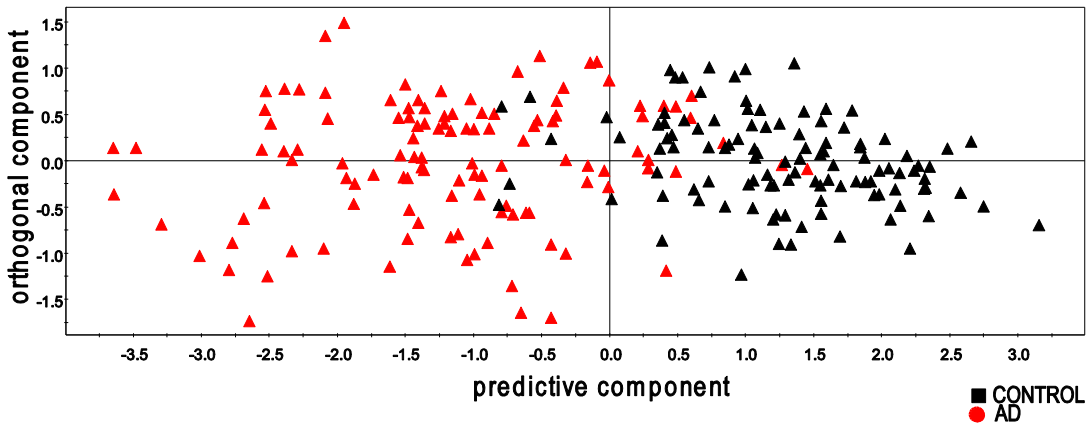

Figure 15. Scatter plot illustrating a significant separation between subjects with Alzheimer's disease and healthy volunteers combining all the MR-measures

Different OPLS models were created to distinguish between AD vs. CTL, AD vs. MCI and MCI vs. CTL using each of the measures separately and together. The greatest significant separation was observed between the groups AD and CTL (Q^2=0.63) when combining all the measures together. We also observed significant separations between AD vs. MCI (Q^2=0.31) and MCI vs. CTL (Q^2=0.29). Comparing AD with CTL we found a sensitivity of 88% and a specificity of 95% (Figure 15). Distinguishing between AD and MCI resulted in a sensitivity of 76% and a specificity of 77% while comparing MCI and. controls yielded a sensitivity of 67% and a specificity of 81%. Combining automated regional volume measures, regional cortical thickness measures and manual outlining of hippocampi together gave higher sensitivity and specificity than using any of the measures alone. Using the different measures separately, manual segmentation of the hippocampus gave the best predictive results. This is however not so surprising since manual measures of the hippocampus are regarded as being "the golden standard" for the early diagnosis of AD with regard to MRI measures. This also highlights the value of manual outlining of the hippocampus. We used the positive

likelihood ratio (LR+) to determine how well the different models performed. The likelihood ratio incorporates both the sensitivity and specificity of a test and provides a direct estimate of how much a test result will change the odds of having a disease. The likelihood ratio for a positive result (LR+) describes how much the odds of getting the disease increase when a test is positive**.** By using manual hippocampal measures alone (AD vs. CTL), yielded in a LR+=9 (a likelihood ratio of 5-10 increases the diagnostic value moderately) but combining the different MRI measures resulted in the LR+ doubling to the value of 18 (a value above 10 significantly increases the diagnostic value of the test). This demonstrates that the regional cortical volumes and the regional cortical thickness measures have an additional diagnostic value. Combining measures and looking at patterns of atrophy has greater diagnostic value than looking at single measures. Manual measures of hippocampal volume, regional volumes of temporal gray matter and entorhinal cortical thickness were particularly important for the separation of the different groups.

This method shows potential for distinguishing between different patient groups and identifying possible markers of disease. Combining the different MRI measures together resulted in significantly better classification than using them separately. Since disease-related patterns of atrophy could be observed, we believe that this method also has potential application in distinguishing between different types of dementias.

7.2.2 Study IV

Study III demonstrated the power of multivariate data analysis in distinguishing between different patient groups. Combining different MRI measures had greater predicative power than using them separately. One of the measures incorporated into the models in study III was hippocampal volumes which were manually outlined. The task of manual outlining is very time-consuming and not practical in clinical practice. Consequently, we only wanted to use automated measures in this study. The use of automated measures may have advantages in particular when it comes to widespread uptake in either clinical or research practice. The major aim of this study was to explore the value of MRS as a complement to automated MRI measures in the diagnosis of AD.

Multivariate data analysis (OPLS) was used to investigate the discrimination between AD and elderly control subjects using MRI measures combined with MRS measures. Three different models were created to distinguish between AD and CTL. In the first multivariate model MRI measures were used alone (Q^2=0.64), the second model contained MRS measures (Q^2=0.34) and the third model combined the two (Q^2=0.71).

Combing MRI and MRS measures (Figure 16) resulted in a sensitivity of 97% and a specificity of 94% compared to using MRI measures alone which yielded a sensitivity of 93% and a specificity of 86% and MRS measures alone resulted in a sensitivity of 76% and a specificity of 82%. Adding the MRS measures more than doubled the positive likelihood ratio from 7 to 16. Examples of measures of importance are regional volumes of hippocampus, amygdala, total gray matter, total CSF and the metabolite NAA. This method shows potential for distinguishing between different patient groups and combining MRI and MRS measures together and resulted in significantly better classification than using them separately, which demonstrates the value of MRS in the early diagnosis of AD.

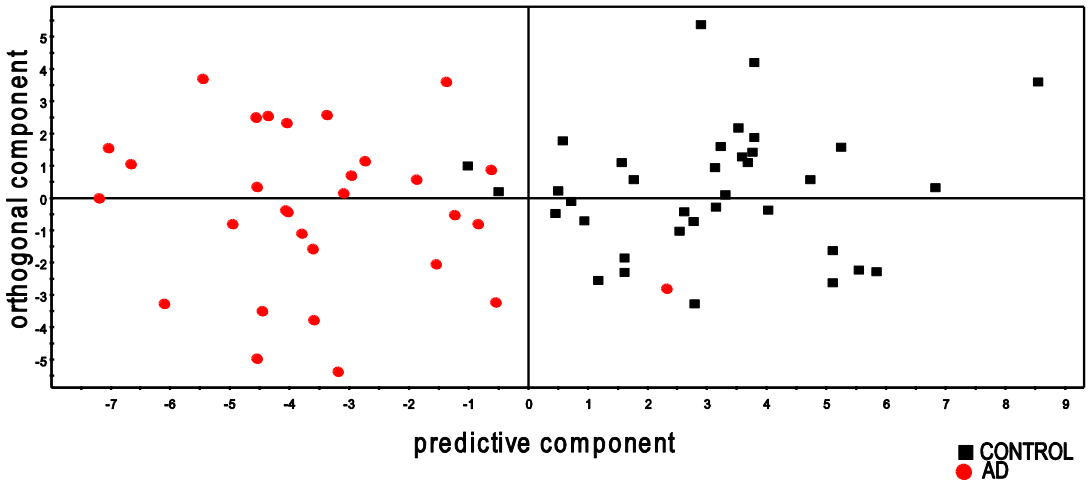

Figure 16. Scatter plot illustrating a significant separation between subjects with Alzheimer's disease and healthy volunteers using both MRI and MRS measures in the model

8 CONCLUSIONS AND FUTURE PERSPECTIVES

The aim of this thesis was to investigate the potential use of combining magnetic resonance imaging and spectroscopy to monitor disease and treatment effects in Alzheimer's disease. Many studies have focused on finding one biomarker of disease, but due to the complexity and heterogeneity of AD, this is probably not possible and the combination of different measures and biomarkers has to be considered. However, general opinion is changing towards combining different measures. By combining different measures or biomarkers using multivariate data analysis, patterns of disease can be revealed. These patterns can be used as new biomarkers in making the diagnosis of AD.

It is most likely that a single structure or metabolite is not sufficient to distinguish between subjects with AD, those with MCI and healthy controls due to the complexity of the disease. The combination of different structures and different types of measures may prove to be more useful in the early detection of MCI and AD. Since patterns of disease are considered, this also gives us the opportunity to distinguish between different disorders, which would not have been possible when looking at single measures. Furthermore, it is of great importance to consider different patterns when monitoring treatment effects. To be able to observe short term treatment effects, especially with the drugs available today combining different MR-measures is of high importance. This thesis deals with the combination of MRI and MRS with multivariate analysis, but adding other measures such as PET and CSF markers is likely to improve the ability to monitor both effects of treatment and disease.

We have shown that it is possible to monitor treatment effects and disease in animal models, as well as to monitor disease in patients combining MRI and MRS with multivariate data analysis. Combining different measures of atrophy improves the predictive ability of the models. By adding MRS, the model predictability also improves, which highlights the value of this technique for early diagnosis.

Looking ahead, these methods will be used longitudinally in patients. The data presented in study III were at baseline and the same patients have been followed at both three and twelve months. By following the same patients longitudinally we can test the robustness of the models and investigate how the disease progresses both in the MCI patients and AD patients. Another important step is to further investigate the MCI group. This is a very heterogeneous group and needs to be further characterized. To be able to observe patterns of the disease, which can determine which subject will convert

to AD, is one of the major aims. Furthermore, to be able to evaluate these methods in a treatment study is another major aim, to combine different MR-measures with multivariate data analysis to find new markers for disease-modifying treatments.

To conclude, the results presented in this thesis show the potential of combining MRI and MRS with multivariate data analysis to monitor both treatment effects and disease progression. The methods are far from perfect but show great potential and may someday be used in clinical practice to diagnosticate AD in an early stage. Furthermore, these methods may be used in clinical trials to assist in the development of new drugs. MRI-examinations are today an integrated part of routine clinical work. For this reason these techniques can be widely used and large patient data can be obtained to create robust models. Finally, patterns of atrophy are considered rather than single structures. This will help to distinguish between different neurological disorders since patterns may be more disease specific.

9 ACKNOWLEDGEMENTS

Finally, I would like to take the opportunity to thank all the people that have helped, guided and encouraged me during my thesis work. I want to thank people from the department of Neurobiology, Care Sciences and Society, the Experimental MR Research Center and MRC at Karolinska Institutet. I also want to thank members of the AddNeuroMed consortium and Swedish Brain Power.

Professor Lars-Olof Wahlund, my main supervisor for guiding me through these years, always being there to help and taking the time to listen. You have always pushed me to work hard and at the same time giving me the freedom to work independently. The combination of freedom and support has made these years educational and interesting.

Professor Christian Spenger for introducing me to the world of research. For always giving me support and help. I have had the opportunity to learn many new things and to meet a lot of interesting people thanks to you.

Docent Ivan Bednar for teaching me most of what I know of about animal care and for all the fun at the Experimental MR Research Center

Teknologi doktor Tomas Klason for introducing me to the world of MRI and MRS

Anette Eidehall for always helping me and for nice conversations.

Andrew Simmons, **Simon Lovestone** and **Hilkka Soininen** and the rest of the AddNeuroMed consortium for support and scientific discussions.

Friends and colleagues at the Karolinska Institutet, especially all my fellow **PhD students** for great conversations in the lunch room, tough training sessions in the gym and many laughs during after work hours. I could mention you all by name, but the list would be very long.

Sebastian Muehlboeck for fruitful collaboration within the AddNeuroMed project and for all fun and memorable times in Montreal.

Johan Lundström for being my Swedish supportive compatriot (vapendragare) during my stay in Montreal.

Karin Jensen for your company during thesis writing and for your friendship.

I also want to thank my friends **Palle**, **B1**, **Matte**, **Peter**, **Jocke** and **Pablo** for all the scientific discussions about everything not related to actual science.

Musse for being a great friend and advisor.

Finally I would like to thank my family, My **Mom (Gullan)**, my **Dad (Lasse)**, my **Sister (Eva)** and my **Brother (Peta)**. You have all always being there to help, comfort and support me. I could not have done this without you.

The AddNeuroMed study is part of InnoMed, a European Union funded FP6 project funded sponsored by EFPIA.

10 REFERENCES

1. Wimo A, Winblad B, Jönsson L. An estimate of the total worldwide societal costs of dementia in 2005. *Alzheimer's and Dementia.* 2007;3(2):81-91.

2. Brookmeyer R, Johnson E, Ziegler-Graham K, Arrighi HM. Forecasting the global burden of Alzheimer's disease. *Alzheimer's and Dementia.* 2007;3(3):186-191.

3. Lovestone S, Francis P, Strandgaard K. Biomarkers for disease modification trials--the innovative medicines initiative and AddNeuroMed. *J Nutr Health Aging.* Jul-Aug 2007;11(4):359-361.

4. Scahill RI, Fox NC. Longitudinal imaging in dementia. *Br J Radiol.* Dec 2007;80 Spec No 2:S92-98.

5. Pearson K. On Lines and Planes of Closest Fit to Systems of Points in Space. *Philosophical Magazine.* 1901;2(6):559-572.

6. Wold S, Ruhe A, Wold H, Dunn WJ, Iii. The Collinearity Problem in Linear Regression. The Partial Least Squares (PLS) Approach to Generalized Inverses. *SIAM Journal on Scientific and Statistical Computing.* 1984;5(3):735-743.

7. Wold S, Trygg J, Berglund A, Antti H. Some recent developments in PLS modeling. *Chemometrics and Intelligent Laboratory Systems.* 2001;58(2):131-150.

8. Johan Trygg SW. Orthogonal projections to latent structures (O-PLS). *Journal of Chemometrics.* 2002;16(3):119-128.

9. Wiklund S, Johansson E, Sjostrom L, et al. Visualization of GC/TOF-MS-based metabolomics data for identification of biochemically interesting compounds using OPLS class models. *Anal Chem.* Jan 1 2008;80(1):115-122.

10. Glenner GG, Wong CW. Alzheimer's disease: initial report of the purification and characterization of a novel cerebrovascular amyloid protein. *Biochem Biophys Res Commun.* May 16 1984;120(3):885-890.

11. Masters CL, Simms G, Weinman NA, Multhaup G, McDonald BL, Beyreuther K. Amyloid plaque core protein in Alzheimer disease and Down syndrome. *Proc Natl Acad Sci U S A.* Jun 1985;82(12):4245-4249.

12. Goedert M, Spillantini MG, Crowther RA. Tau proteins and neurofibrillary degeneration. *Brain Pathol.* Jul 1991;1(4):279-286.

13. Corder EH, Saunders AM, Strittmatter WJ, et al. Gene dose of apolipoprotein E type 4 allele and the risk of Alzheimer's disease in late onset families. *Science.* Aug 13 1993;261(5123):921-923.

14. Wisniewski T, Castano EM, Golabek A, Vogel T, Frangione B. Acceleration of Alzheimer's fibril formation by apolipoprotein E in vitro. *Am J Pathol.* Nov 1994;145(5):1030-1035.

15. Goate A, Chartier-Harlin MC, Mullan M, et al. Segregation of a missense mutation in the amyloid precursor protein gene with familial Alzheimer's disease. *Nature.* Feb 21 1991;349(6311):704-706.

16. Sherrington R, Rogaev EI, Liang Y, et al. Cloning of a gene bearing missense mutations in early-onset familial Alzheimer's disease. *Nature.* Jun 29 1995;375(6534):754-760.

17. Levy-Lahad E, Wijsman EM, Nemens E, et al. A familial Alzheimer's disease locus on chromosome 1. *Science.* Aug 18 1995;269(5226):970-973.

18. Selkoe DJ. Alzheimer's disease: genes, proteins, and therapy. *Physiol Rev.* Apr 2001;81(2):741-766.

19. Selkoe DJ. The molecular pathology of Alzheimer's disease. *Neuron.* Apr 1991;6(4):487-498.

20. Lambert MP, Barlow AK, Chromy BA, et al. Diffusible, nonfibrillar ligands derived from Abeta1-42 are potent central nervous system neurotoxins. *Proc Natl Acad Sci U S A.* May 26 1998;95(11):6448-6453.

21. Takahashi RH, Almeida CG, Kearney PF, et al. Oligomerization of Alzheimer's beta-amyloid within processes and synapses of cultured neurons and brain. *J Neurosci.* Apr 7 2004;24(14):3592-3599.

22. Walsh DM, Tseng BP, Rydel RE, Podlisny MB, Selkoe DJ. The oligomerization of amyloid beta-protein begins intracellularly in cells derived from human brain. *Biochemistry.* Sep 5 2000;39(35):10831-10839.

23. Chiang PK, Lam MA, Luo Y. The many faces of amyloid beta in Alzheimer's disease. *Curr Mol Med.* Sep 2008;8(6):580-584.

24. Hardy J, Selkoe DJ. The amyloid hypothesis of Alzheimer's disease: progress and problems on the road to therapeutics. *Science.* Jul 19 2002;297(5580):353-356.

25. Braak H, Braak E. Neuropathological stageing of Alzheimer-related changes. *Acta Neuropathologica.* 1991;82(4):239-259.

26. McKhann G, Drachman D, Folstein M, Katzman R, Price D, Stadlan EM. Clinical diagnosis of Alzheimer's disease: report of the NINCDS-ADRDA Work Group under the auspices of Department of Health and Human Services Task Force on Alzheimer's Disease. *Neurology.* Jul 1984;34(7):939-944.

27. Folstein MF, Folstein SE, McHugh PR. "Mini-mental state". A practical method for grading the cognitive state of patients for the clinician. *J Psychiatr Res.* Nov 1975;12(3):189-198.

28. Hughes CP, Berg L, Danziger WL, Coben LA, Martin RL. A new clinical scale for the staging of dementia. *Br J Psychiatry.* Jun 1982;140:566-572.

29. Rosen WG, Mohs RC, Davis KL. A new rating scale for Alzheimer's disease. *Am J Psychiatry.* Nov 1984;141(11):1356-1364.

30. Dubois B. Interest of the new criteria for drug trials in AD. *The Journal of Nutrition, Health and Aging.* 2009;13(4):356-357.

31. Dubois B, Feldman HH, Jacova C, et al. Research criteria for the diagnosis of Alzheimer's disease: revising the NINCDS-ADRDA criteria. *The Lancet Neurology.* 2007;6(8):734-746.

32. Petersen RC, Smith GE, Waring SC, Ivnik RJ, Tangalos EG, Kokmen E. Mild Cognitive Impairment: Clinical Characterization and Outcome. *Arch Neurol.* March 1, 1999 1999;56(3):303-308.

33. Visser PJ, Scheltens P, Verhey FR. Do MCI criteria in drug trials accurately identify subjects with predementia Alzheimer's disease? *J Neurol Neurosurg Psychiatry.* Oct 2005;76(10):1348-1354.

34. Kantarci K. Magnetic resonance markers for early diagnosis and progression of Alzheimer's disease. *Expert Rev Neurother.* Sep 2005;5(5):663-670.

35. Winblad B, Palmer K, Kivipelto M, et al. Mild cognitive impairment – beyond controversies, towards a consensus: report of the International Working Group on Mild Cognitive Impairment. *Journal of Internal Medicine.* 2004;256(3):240-246.

36. O'Brien JT. Role of imaging techniques in the diagnosis of dementia. *Br J Radiol.* Dec 2007;80 Spec No 2:S71-77.

37. Ries ML, Carlsson CM, Rowley HA, et al. Magnetic resonance imaging characterization of brain structure and function in mild cognitive impairment: a review. *J Am Geriatr Soc.* May 2008;56(5):920-934.

38. Fox NC, Warrington EK, Freeborough PA, et al. Presymptomatic hippocampal atrophy in Alzheimer's disease. A longitudinal MRI study. *Brain.* Dec 1996;119 (Pt 6):2001-2007.

39. Jack CR, Jr., Petersen RC, O'Brien PC, Tangalos EG. MR-based hippocampal volumetry in the diagnosis of Alzheimer's disease. *Neurology.* Jan 1992;42(1):183-188.

40. Jack CR, Jr., Petersen RC, Xu YC, et al. Medial temporal atrophy on MRI in normal aging and very mild Alzheimer's disease. *Neurology.* Sep 1997;49(3):786-794.

41. Juottonen K, Laakso MP, Partanen K, Soininen H. Comparative MR analysis of the entorhinal cortex and hippocampus in diagnosing Alzheimer disease. *AJNR Am J Neuroradiol.* Jan 1999;20(1):139-144.

42. Killiany RJ, Moss MB, Albert MS, Sandor T, Tieman J, Jolesz F. Temporal lobe regions on magnetic resonance imaging identify patients with early Alzheimer's disease. *Arch Neurol.* Sep 1993;50(9):949-954.

43. Laakso MP, Partanen K, Riekkinen P, et al. Hippocampal volumes in Alzheimer's disease, Parkinson's disease with and without dementia, and in vascular dementia: An MRI study. *Neurology.* Mar 1996;46(3):678-681.

44. Laakso MP, Soininen H, Partanen K, et al. MRI of the hippocampus in Alzheimer's disease: sensitivity, specificity, and analysis of the incorrectly classified subjects. *Neurobiol Aging.* Jan-Feb 1998;19(1):23-31.

45. Lehericy S, Baulac M, Chiras J, et al. Amygdalohippocampal MR volume measurements in the early stages of Alzheimer disease. *AJNR Am J Neuroradiol.* May 1994;15(5):929-937.

46. Seab JP, Jagust WJ, Wong ST, Roos MS, Reed BR, Budinger TF. Quantitative NMR measurements of hippocampal atrophy in Alzheimer's disease. *Magn Reson Med.* Oct 1988;8(2):200-208.

47. Xu Y, Jack CR, Jr., O'Brien PC, et al. Usefulness of MRI measures of entorhinal cortex versus hippocampus in AD. *Neurology.* May 9 2000;54(9):1760-1767.

48. Chetelat G, Landeau B, Eustache F, et al. Using voxel-based morphometry to map the structural changes associated with rapid conversion in MCI: a longitudinal MRI study. *Neuroimage.* Oct 1 2005;27(4):934-946.

49. Davies R, Scahill V, Graham A, Williams G, Graham K, Hodges J. Development of an MRI rating scale for multiple brain regions: comparison with volumetrics and with voxel-based morphometry. *Neuroradiology.* 2008;51(8):491-503.

50. Drzezga A, Grimmer T, Henriksen G, et al. Effect of APOE genotype on amyloid plaque load and gray matter volume in Alzheimer disease. *Neurology.* April 28, 2009 2009;72(17):1487-1494.

51. Waragai M, Okamura N, Furukawa K, et al. Comparison study of amyloid PET and voxel-based morphometry analysis in mild cognitive impairment and Alzheimer's disease. *Journal of the Neurological Sciences.*In Press, Corrected Proof.

52. Teipel SJ, Born C, Ewers M, et al. Multivariate deformation-based analysis of brain atrophy to predict Alzheimer's disease in mild cognitive impairment. *Neuroimage.* 2007;38(1):13-24.

53. Lerch JP, Evans AC. Cortical thickness analysis examined through power analysis and a population simulation. *Neuroimage.* Jan 1 2005;24(1):163-173.

54. Lerch JP, Pruessner J, Zijdenbos AP, et al. Automated cortical thickness measurements from MRI can accurately separate Alzheimer's patients from normal elderly controls. *Neurobiol Aging.* Jan 2008;29(1):23-30.

55. McEvoy LK, Fennema-Notestine C, Roddey JC, et al. Alzheimer Disease: Quantitative Structural Neuroimaging for Detection and Prediction of Clinical and Structural Changes in Mild Cognitive Impairment. *Radiology.* February 6, 2009 2009:2511080924.

56. Kantarci K. 1H magnetic resonance spectroscopy in dementia. *Br J Radiol.* Dec 2007;80 Spec No 2:S146-152.

57. Miller BL, Moats RA, Shonk T, Ernst T, Woolley S, Ross BD. Alzheimer disease: depiction of increased cerebral myo-inositol with proton MR spectroscopy. *Radiology.* May 1993;187(2):433-437.

58. Adalsteinsson E, Sullivan EV, Kleinhans N, Spielman DM, Pfefferbaum A. Longitudinal decline of the neuronal marker N-acetyl aspartate in Alzheimer's disease. *Lancet.* May 13 2000;355(9216):1696-1697.

59. Moats RA, Ernst T, Shonk TK, Ross BD. Abnormal cerebral metabolite concentrations in patients with probable Alzheimer disease. *Magn Reson Med.* Jul 1994;32(1):110-115.

60. Dixon RM, Bradley KM, Budge MM, Styles P, Smith AD. Longitudinal quantitative proton magnetic resonance spectroscopy of the hippocampus in Alzheimer's disease. *Brain.* Oct 2002;125(Pt 10):2332-2341.

61. Schuff N, Amend D, Ezekiel F, et al. Changes of hippocampal N-acetyl aspartate and volume in Alzheimer's disease. A proton MR spectroscopic imaging and MRI study. *Neurology.* Dec 1997;49(6):1513-1521.

62. Kantarci K, Jack CR, Jr., Xu YC, et al. Regional metabolic patterns in mild cognitive impairment and Alzheimer's disease: A 1H MRS study. *Neurology.* Jul 25 2000;55(2):210-217.

63. Kantarci K, Weigand SD, Przybelski SA, et al. Risk of dementia in MCI: Combined effect of cerebrovascular disease, volumetric MRI, and 1H MRS. *Neurology.* April 28, 2009 2009;72(17):1519-1525.

64. Marjanska M, Curran GL, Wengenack TM, et al. Monitoring disease progression in transgenic mouse models of Alzheimer's disease with proton magnetic resonance spectroscopy. *Proc Natl Acad Sci U S A.* Aug 16 2005;102(33):11906-11910.

65. Rupsingh R, Borrie M, Smith M, Wells JL, Bartha R. Reduced hippocampal glutamate in Alzheimer disease. *Neurobiol Aging.* Jun 5 2009.

66. Firbank MJ, Harrison RM, O'Brien JT. A comprehensive review of proton magnetic resonance spectroscopy studies in dementia and Parkinson's disease. *Dement Geriatr Cogn Disord.* 2002;14(2):64-76.

67. Ross BD, Bluml S, Cowan R, Danielsen E, Farrow N, Gruetter R. In vivo magnetic resonance spectroscopy of human brain: the biophysical basis of dementia. *Biophys Chem.* Oct 1997;68(1-3):161-172.

68. den Heijer T, Sijens PE, Prins ND, et al. MR spectroscopy of brain white matter in the prediction of dementia. *Neurology.* Feb 28 2006;66(4):540-544.

69. Chepkova AN, Doreulee N, Yanovsky Y, Mukhopadhyay D, Haas HL, Sergeeva OA. Long-lasting enhancement of corticostriatal neurotransmission by taurine. *Eur J Neurosci.* Oct 2002;16(8):1523-1530.

70. Dedeoglu A, Choi JK, Cormier K, Kowall NW, Jenkins BG. Magnetic resonance spectroscopic analysis of Alzheimer's disease mouse brain that express mutant human APP shows altered neurochemical profile. *Brain Res.* Jun 25 2004;1012(1-2):60-65.

71. Reisberg B, Doody R, Stoffler A, Schmitt F, Ferris S, Mobius HJ. A 24-week open-label extension study of memantine in moderate to severe Alzheimer disease. *Arch Neurol.* Jan 2006;63(1):49-54.

72. Hartmann S, Mobius HJ. Tolerability of memantine in combination with cholinesterase inhibitors in dementia therapy. *Int Clin Psychopharmacol.* Mar 2003;18(2):81-85.

73. Seltzer B. Donepezil: a review. *Expert Opin Drug Metab Toxicol.* Oct 2005;1(3):527-536.

74. Cummings JL. Use of cholinesterase inhibitors in clinical practice: evidence-based recommendations. *Am J Geriatr Psychiatry.* Mar-Apr 2003;11(2):131-145.

75. Borkowska A, Ziolkowska-Kochan M, Rybakowski JK. One-year treatment of Alzheimer's disease with acetylcholinesterase inhibitors: improvement on ADAS-cog and TMT A, no change or worsening on other tests. *Hum Psychopharmacol.* Aug 2005;20(6):409-414.

76. Krishnan KR, Charles HC, Doraiswamy PM, et al. Randomized, placebo-controlled trial of the effects of donepezil on neuronal markers and hippocampal volumes in Alzheimer's disease. *Am J Psychiatry.* Nov 2003;160(11):2003-2011.

77. Jessen F, Traeber F, Freymann K, Maier W, Schild HH, Block W. Treatment monitoring and response prediction with proton MR spectroscopy in AD. *Neurology.* Aug 8 2006;67(3):528-530.

78. Bartha R, Smith M, Rupsingh R, Rylett J, Wells JL, Borrie MJ. High field (1)H MRS of the hippocampus after donepezil treatment in Alzheimer disease. *Prog Neuropsychopharmacol Biol Psychiatry.* Apr 1 2008;32(3):786-793.

79. Westman E, Spenger C, Oberg J, Reyer H, Pahnke J, Wahlund LO. In vivo 1H-magnetic resonance spectroscopy can detect metabolic changes in APP/PS1 mice after donepezil treatment. *BMC Neurosci.* 2009;10:33.

80. Codita A, Winblad B, Mohammed AH. Of mice and men: more neurobiology in dementia. *Curr Opin Psychiatry.* Nov 2006;19(6):555-563.

81. Games D, Buttini M, Kobayashi D, Schenk D, Seubert P. Mice as models: transgenic approaches and Alzheimer's disease. *J Alzheimers Dis.* 2006;9(3 Suppl):133-149.

82. Higgins GA, Jacobsen H. Transgenic mouse models of Alzheimer's disease: phenotype and application. *Behav Pharmacol.* Sep 2003;14(5-6):419-438.

83. Kobayashi DT, Chen KS. Behavioral phenotypes of amyloid-based genetically modified mouse models of Alzheimer's disease. *Genes Brain Behav.* Apr 2005;4(3):173-196.

84. Van Dam D, De Deyn PP. Drug discovery in dementia: the role of rodent models. *Nat Rev Drug Discov.* Nov 2006;5(11):956-970.

85. Borchelt DR, Ratovitski T, van Lare J, et al. Accelerated amyloid deposition in the brains of transgenic mice coexpressing mutant presenilin 1 and amyloid precursor proteins. *Neuron.* Oct 1997;19(4):939-945.

86. Games D, Adams D, Alessandrini R, et al. Alzheimer-type neuropathology in transgenic mice overexpressing V717F beta-amyloid precursor protein. *Nature.* Feb 9 1995;373(6514):523-527.

87. Lewis J, Dickson DW, Lin WL, et al. Enhanced neurofibrillary degeneration in transgenic mice expressing mutant tau and APP. *Science.* Aug 24 2001;293(5534):1487-1491.

88. Oddo S, Caccamo A, Shepherd JD, et al. Triple-transgenic model of Alzheimer's disease with plaques and tangles: intracellular Abeta and synaptic dysfunction. *Neuron.* Jul 31 2003;39(3):409-421.

89. Duff K, Eckman C, Zehr C, et al. Increased amyloid-beta42(43) in brains of mice expressing mutant presenilin 1. *Nature.* Oct 24 1996;383(6602):710-713.

90. Holcomb L, Gordon MN, McGowan E, et al. Accelerated Alzheimer-type phenotype in transgenic mice carrying both mutant amyloid precursor protein and presenilin 1 transgenes. *Nat Med.* Jan 1998;4(1):97-100.

91. Donahue LR, Cook SA, Johnson KR, Bronson RT, Davisson MT. Megencephaly: a new mouse mutation on chromosome 6 that causes hypertrophy of the brain. *Mamm Genome.* Dec 1996;7(12):871-876.

92. Petersson S, Persson AS, Johansen JE, et al. Truncation of the Shaker-like voltage-gated potassium channel, Kv1.1, causes megencephaly. *Eur J Neurosci.* Dec 2003;18(12):3231-3240.

93. Diez M, Schweinhardt P, Petersson S, et al. MRI and in situ hybridization reveal early disturbances in brain size and gene expression in the megencephalic (mceph/mceph) mouse. *Eur J Neurosci.* Dec 2003;18(12):3218-3230.

94. Petersson S, Lavebratt C, Schalling M, Hokfelt T. Expression of cholecystokinin, enkephalin, galanin and neuropeptide Y is markedly changed in the brain of the megencephaly mouse. *Neuroscience.* 2000;100(2):297-317.

95. Sled JG, Zijdenbos AP, Evans AC. A nonparametric method for automatic correction of intensity nonuniformity in MRI data. *IEEE Trans Med Imaging.* Feb 1998;17(1):87-97.

96. Cocosco CA, Zijdenbos AP, Evans AC. A fully automatic and robust brain MRI tissue classification method. *Med Image Anal.* Dec 2003;7(4):513-527.

97. Zijdenbos AP, Forghani R, Evans AC. Automatic "pipeline" analysis of 3-D MRI data for clinical trials: application to multiple sclerosis. *IEEE Trans Med Imaging.* Oct 2002;21(10):1280-1291.

98. Collins DL, Neelin P, Peters TM, Evans AC. Automatic 3D intersubject registration of MR volumetric data in standardized Talairach space. *J Comput Assist Tomogr.* Mar-Apr 1994;18(2):192-205.

99. D. Louis Collins CJHTMPACE. Automatic 3-D model-based neuroanatomical segmentation. *Human Brain Mapping.* 1995;3(3):190-208.

100. Segonne F, Dale AM, Busa E, et al. A hybrid approach to the skull stripping problem in MRI. *Neuroimage.* Jul 2004;22(3):1060-1075.

101. Fischl B, Salat DH, Busa E, et al. Whole brain segmentation: automated labeling of neuroanatomical structures in the human brain. *Neuron.* Jan 31 2002;33(3):341-355.

102. Fischl B, Salat DH, van der Kouwe AJ, et al. Sequence-independent segmentation of magnetic resonance images. *Neuroimage.* 2004;23 Suppl 1:S69-84.

103. Fischl B, Liu A, Dale AM. Automated manifold surgery: constructing geometrically accurate and topologically correct models of the human cerebral cortex. *IEEE Trans Med Imaging.* Jan 2001;20(1):70-80.

104. Segonne F, Pacheco J, Fischl B. Geometrically accurate topology-correction of cortical surfaces using nonseparating loops. *IEEE Trans Med Imaging.* Apr 2007;26(4):518-529.

105. Dale AM, Fischl B, Sereno MI. Cortical surface-based analysis. I. Segmentation and surface reconstruction. *Neuroimage.* Feb 1999;9(2):179-194.

106. Dale AM, Sereno MI. Improved Localizadon of Cortical Activity by Combining EEG and MEG with MRI Cortical Surface Reconstruction: A Linear Approach. *Journal of Cognitive Neuroscience.* 1993;5(2):162-176.

107. Fischl B, Dale AM. Measuring the thickness of the human cerebral cortex from magnetic resonance images. *Proc Natl Acad Sci U S A.* Sep 26 2000;97(20):11050-11055.

108. Fischl B, Sereno MI, Dale AM. Cortical surface-based analysis. II: Inflation, flattening, and a surface-based coordinate system. *Neuroimage.* Feb 1999;9(2):195-207.

109. Fischl B, Sereno MI, Tootell RB, Dale AM. High-resolution intersubject averaging and a coordinate system for the cortical surface. *Hum Brain Mapp.* 1999;8(4):272-284.

110. Desikan RS, Ségonne F, Fischl B, et al. An automated labeling system for subdividing the human cerebral cortex on MRI scans into gyral based regions of interest. *NeuroImage.* 2006;31(3):968-980.

111. Fischl B, van der Kouwe A, Destrieux C, et al. Automatically parcellating the human cerebral cortex. *Cereb Cortex.* Jan 2004;14(1):11-22.

112. Pantel J, O'Leary DS, Cretsinger K, et al. A new method for the in vivo volumetric measurement of the human hippocampus with high neuroanatomical accuracy. *Hippocampus.* 2000;10(6):752-758.

113. Provencher SW. Estimation of metabolite concentrations from localized in vivo proton NMR spectra. *Magn Reson Med.* Dec 1993;30(6):672-679.

114. Provencher SW. Automatic quantitation of localized in vivo 1H spectra with LCModel. *NMR Biomed.* Jun 2001;14(4):260-264.

115. Ackl N, Ising M, Schreiber YA, Atiya M, Sonntag A, Auer DP. Hippocampal metabolic abnormalities in mild cognitive impairment and Alzheimer's disease. *Neurosci Lett.* Aug 12-19 2005;384(1-2):23-28.

116. Westman E, Spenger C, Wahlund LO, Lavebratt C. Carbamazepine treatment recovered low N-acetylaspartate+N-acetylaspartylglutamate (tNAA) levels in the megencephaly mouse BALB/cByJ-Kv1.1(mceph/mceph). *Neurobiol Dis.* Apr 2007;26(1):221-228.

117. Eriksson L, Johansson E, Kettaneh-Wold N, Trygg J, Wiksröm C, Wold S. *Multi- and Megavariate Data Analysis (Part I -Basics and Principals and Applications)*. 2nd ed. Umeå: Umetrics AB; 2006.

118. Hye A, Lynham S, Thambisetty M, et al. Proteome-based plasma biomarkers for Alzheimer's disease. *Brain.* Nov 2006;129(Pt 11):3042-3050.

119. Jack CR, Jr., Bernstein MA, Fox NC, et al. The Alzheimer's Disease Neuroimaging Initiative (ADNI): MRI methods. *J Magn Reson Imaging.* Apr 2008;27(4):685-691.

120. Lavebratt C, Trifunovski A, Persson AS, et al. Carbamazepine protects against megencephaly and abnormal expression of BDNF and Nogo signaling components in the mceph/mceph mouse. *Neurobiol Dis.* Sep 19 2006.

121. Chernov MF, Kubo O, Hayashi M, et al. Proton MRS of the peritumoral brain. *J Neurol Sci.* Feb 15 2005;228(2):137-142.

122. Flugel D, McLean MA, Simister RJ, Duncan JS. Magnetisation transfer ratio of choline is reduced following epileptic seizures. *NMR Biomed.* Apr 2006;19(2):217-222.

123. Lee SK, Kim DW, Kim KK, Chung CK, Song IC, Chang KH. Effect of seizure on hippocampus in mesial temporal lobe epilepsy and neocortical epilepsy: an MRS study. *Neuroradiology.* Dec 2005;47(12):916-923.

124. Riederer F, Bittsansky M, Schmidt C, et al. 1H magnetic resonance spectroscopy at 3 T in cryptogenic and mesial temporal lobe epilepsy. *NMR Biomed.* Aug 2006;19(5):544-553.

125. Groeschel S, Brockmann K, Dechent P, Wilichowski E, Frahm J, Hanefeld F. Magnetic resonance imaging and proton magnetic resonance spectroscopy of

megalencephaly and dilated Virchow-Robin spaces. *Pediatr Neurol.* Jan 2006;34(1):35-40.

126. Muramatsu M, Kakita K, Nakagawa K, Kuriyama K. A modulating role of taurine on release of acetylcholine and norepinephrine from neuronal tissues. *Jpn J Pharmacol.* Apr 1978;28(2):259-268.

127. Kantarci K, Petersen RC, Boeve BF, et al. 1H MR spectroscopy in common dementias. *Neurology.* Oct 26 2004;63(8):1393-1398.